

CERN-EP-2020-119
29 June 2020

Observation of enhanced double parton scattering in proton-lead collisions at $\sqrt{s_{\text{NN}}} = 8.16 \text{ TeV}$

LHCb collaboration[†]

Abstract

A study of prompt charm-hadron pair production in proton-lead collisions at $\sqrt{s_{\text{NN}}} = 8.16 \text{ TeV}$ is performed using data corresponding to an integrated luminosity of about 30 nb^{-1} , collected with the LHCb experiment. Production cross-sections for different pairs of charm hadrons are measured and kinematic correlations between the two charm hadrons are investigated. This is the first measurement of associated production of two charm hadrons in proton-lead collisions. The results confirm the predicted enhancement of double parton scattering in heavy-ion collisions.

Submitted to Phys. Rev. Lett.

© 2020 CERN for the benefit of the LHCb collaboration. CC BY 4.0 licence.

[†]Authors are listed at the end of this paper.

At high energy hadron colliders, particles are produced in fundamental collisions of internal partons in the beam projectiles. The underlying parton densities are described by parton distribution functions (PDFs). The associated production of multiple heavy-flavor hadrons can be generated from a single parton scattering (SPS) or multiple parton scatterings. The latter is necessary for the successful description of large charged-track multiplicities and event-activity-dependent heavy-flavor production [1–4]. In a simple model, assuming that the PDFs of two partons in the same projectile are independent, the associated production cross-section of final-state particles A and B from two separate partonic interactions, *i.e.* a double parton scattering (DPS) process, is related to the inclusive production cross-section of A and B , σ^A and σ^B , as [5–14],

$$\sigma_{\text{DPS}}^{AB} = \frac{1}{1 + \delta_{AB}} \frac{\sigma^A \sigma^B}{\sigma_{\text{eff}}}. \quad (1)$$

Here, $\delta_{AB} = 1$ if A and B are identical and is zero otherwise, and σ_{eff} is the so-called effective cross-section. The parameter σ_{eff} is related to the collision geometry and is expected to be independent of the final state [15–17].

The production of two open charm hadrons, $D_1 D_2$, and $J/\psi D$ meson pairs is of particular interest in the study of SPS and DPS processes. In this Letter, D and $D_{1,2}$ refer to either a D^0 , D^+ or D_s^+ meson and the inclusion of charge conjugate states is implied. Both like-sign (LS) and opposite-sign (OS) open charm hadron pairs are considered. In an LS pair the two hadrons have the same charm-quark flavor, while in an OS pair they have opposite charm flavors. Opposite-sign pairs can be produced from a $c\bar{c}$ pair via SPS, thus the kinematics of the two hadrons are correlated. This correlation may be modified in heavy-ion data compared to proton-proton (pp) collisions, due to nuclear matter effects [18–25]. The OS correlation is predicted to be sensitive to the properties of the hot medium formed in ultra-relativistic heavy nucleus-nucleus collisions [26–36].

The two hadrons in an LS pair produced in a DPS process are expected to be uncorrelated. Studies of LS pair production and correlation in different environments help to test the universality of the parameter σ_{eff} and gain insight into the underlying parton correlations. The ratio of DPS to SPS cross-sections in proton-lead (p -Pb) collisions is estimated to be about three times larger than in pp collisions [10, 37–43]. Since DPS production involves two parton pairs, it is very sensitive to the nuclear PDF (nPDF), including its possible dependence on the position inside the Pb nucleus [44].

Production of OS charm and beauty pairs has been studied in fully reconstructed decays [45–49] and using partially reconstructed decays [50–57], and the hadron and anti-hadron are found to be correlated; in particular, the azimuthal angle, $\Delta\phi$, between the two hadron directions projected to the plane transverse to the beam line favors values close to $\Delta\phi = 0$ or π . Production of LS charm pairs, double quarkonium and multiple jets at the Tevatron and the LHC revealed evidence of DPS signals [49, 58–66]. The effective cross-section is measured to be in the range of 10 to 20 mb for most final states, however, a value as low as 5 mb is extracted using double quarkonium production [67–69]. More measurements are required to resolve this puzzle.

This Letter presents the first measurement of charm pair production in p -Pb collisions at a nucleon-nucleon center-of-mass energy of $\sqrt{s_{\text{NN}}} = 8.16$ TeV. The data were collected with the LHCb experiment at a low interaction rate in two distinct beam configurations. In the p Pb configuration, particles produced in the direction of the proton beam are analysed, while in the Pb p configuration particles are analysed in the Pb beam direction. The p Pb

(Pb p) data correspond to an integrated luminosity of $12.2 \pm 0.3 \text{ nb}^{-1}$ ($18.6 \pm 0.5 \text{ nb}^{-1}$). The detector coordinate system is defined to have the z -axis aligned with the proton beam direction. In the following, particle rapidities (y) are defined in the nucleon-nucleon rest frame.

The LHCb detector is a single-arm forward spectrometer described in detail in Refs. [70, 71]. The online event selection is performed by a trigger, which consists of a hardware stage, based on information from the calorimeter and muon systems, followed by a software stage, which applies a full event reconstruction. Charm hadrons ($H_c \equiv D^0, D^+, D_s^+, J/\psi$) are reconstructed online via the decays $D^0 \rightarrow K^- \pi^+$, $D^+ \rightarrow K^- \pi^+ \pi^+$, $D_s^+ \rightarrow K^- K^+ \pi^+$ and $J/\psi \rightarrow \mu^+ \mu^-$. The data samples are selected by the hardware trigger based on the calorimeter activity for D candidates and based on the muon system for J/ψ candidates. Candidate pairs are formed by $D^0 D^0$, $D^0 \bar{D}^0$ and $D^+ D^\pm$ combinations (same species), and $D^0 D^\pm$, $D^0 D_s^\pm$, $D^+ D_s^\pm$ and $J/\psi D^{0,+}$ combinations (different species). Other charm pairs are not considered due to their limited yield in the data. The tracks used to reconstruct the D mesons are required to be positively identified as kaons or pions and must be separated from every primary p -Pb collision vertex (PV). These tracks are also required to have transverse momentum $p_T > 250 \text{ MeV}/c$ and at least one track must have $p_T > 500 \text{ MeV}/c$ ($p_T > 1000 \text{ MeV}/c$) for D^0 (D^+, D_s^+) final states. The tracks are required to form a vertex of good quality that is separated from every PV. The reconstructed D mesons are required to be consistent with originating from a PV, which favors prompt production over mesons from beauty-hadron decays (denoted as charm-from- b). The two muons used to reconstruct J/ψ candidates are required to have $p_T > 500 \text{ MeV}/c$ and form a good-quality vertex.

In the offline selection, kaons and pions are required to have momentum $p > 3 \text{ GeV}/c$, and muons to have $p > 6 \text{ GeV}/c$, $p_T > 750 \text{ MeV}/c$ and be positively identified by using information from all subdetectors [72, 73]. The $K^- K^+$ invariant mass from the $D_s^+ \rightarrow K^- K^+ \pi^+$ decay is required to be within $\pm 20 \text{ MeV}/c^2$ of the known $\phi(1020)$ mass [74]. A kinematic fit is performed on each charm hadron and on the pair, constraining them to originate from a PV. Requirements on the fit qualities strongly reduce charm-from- b contributions but retain more than 99% of prompt pairs.

Results are obtained in a charm-hadron kinematic region $p_T(H_c) < 12 \text{ GeV}/c$ and $1.7 < y(H_c) < 3.7$ ($-4.7 < y(H_c) < -2.7$) for p Pb (Pb p) data. For D^+ and D_s^+ mesons the requirement $p_T(H_c) > 2 \text{ GeV}/c$ is applied due to extremely small yields at lower p_T . Total cross-sections of $D^0 D^0$, $D^0 \bar{D}^0$ and $J/\psi D^0$ pair production are also evaluated in the full LHCb rapidity acceptance, $1.5 < y(H_c) < 4$ ($-5 < y(H_c) < -2.5$) for p Pb (Pb p) data, in order to compare with single charm production [75, 76].

The cross-section for a charm pair is calculated as $\sigma = N^{\text{corr}}/(\mathcal{L} \times \mathcal{B}_1 \times \mathcal{B}_2)$, where \mathcal{L} is the integrated luminosity, and N^{corr} is the signal yield after efficiency correction and the subtraction of charm-from- b background. The branching fractions of the two charm-hadron decays, $\mathcal{B}_{1,2}$, are taken from Ref. [74] for the D^0 , D^+ , J/ψ decays, and $\mathcal{B}(D_s^+ \rightarrow (K^+ K^-)_\phi \pi^+) = (2.24 \pm 0.13)\%$ from Refs. [77, 78]. The raw signal yield is determined from an unbinned maximum likelihood fit to the distribution of the invariant masses, m_1 and m_2 , of the two charm hadrons. The two-dimensional probability densities comprise four components: signal-signal, background-background, signal-background and background-signal for the first-second charm hadron in a pair. The background is mainly from random combinations of tracks. The signal component for each charm hadron is described by the sum of a Gaussian and a Crystal Ball function (CB) [79]

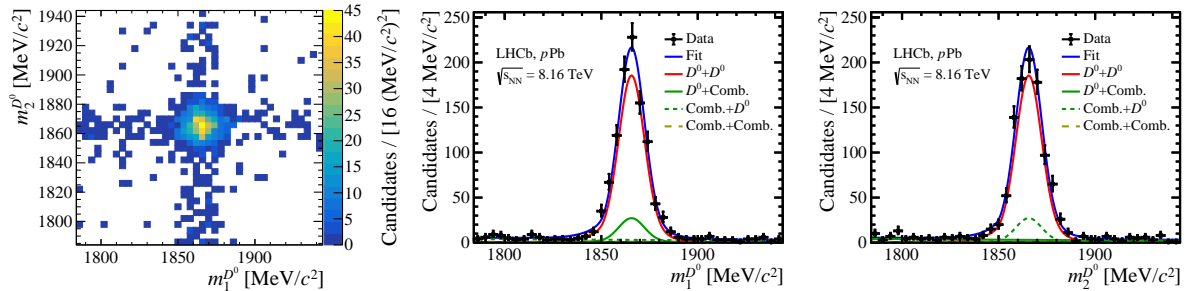


Figure 1: (Left) Two-dimensional invariant-mass distributions of (m_1, m_2) for $D^0 D^0$ pairs and the projections on (middle) m_1 and (right) m_2 with the fit results superimposed. Shown in the projection plots are (points with bars) p Pb data, (solid blue) the total fit and its four components.

and the background component by an exponential function. The distribution for pairs of same-species hadrons is constructed to be independent of the ordering of m_1 and m_2 . As an example, the (m_1, m_2) distribution for $D^0 D^0$ candidates and its projection on m_1 and m_2 are shown in Fig. 1 for p Pb data, with the fit projections overlaid. More distributions are shown in the Supplemental Material. The raw signal yield is between 100 and 4000 for all hadron pairs considered.

The total detection efficiency for each individual charm hadron is evaluated from simulated signal decays, properly corrected using control samples of p -Pb collisions. These control samples are used to calibrate track finding and particle identification (PID) efficiencies [80]. In the simulation, minimum-bias p -Pb collisions are produced using the EPOS generator [81] according to beam configurations of the data. Charm hadrons are generated in pp collisions at $\sqrt{s} = 8.16$ TeV using PYTHIA8 [82, 83] and are embedded into EPOS minimum-bias events. Particle decays are described by EVTGEN [84], while the particle interaction with the detector, and its response, are implemented using the GEANT4 toolkit [85] as described in Ref. [86]. The track finding efficiency in data and simulation is studied with a tag-and-probe method using $J/\psi \rightarrow \mu^+ \mu^-$ decays [87]. Similarly, the PID efficiency is measured using large control samples of $D^0 \rightarrow K^- \pi^+$ and $J/\psi \rightarrow \mu^+ \mu^-$ decays for K^-, π^+ and μ^- tracks, in bins of track momentum and pseudorapidity (p, η) . The average charged-track multiplicity in OS data is similar to the one in the control samples, while for LS data it is about 13% higher, which is consistent with a larger contribution of multiple parton scattering in LS data [1–4]. The corresponding difference in detector occupancy results in different detection efficiencies in LS and OS data, which is evaluated in control samples. Efficiencies from control samples are combined with simulation to obtain the efficiency for each charm hadron as a function of p_T and y , $\epsilon(p_T, y)$, which is used to determine the efficiency corrected signal yield $\sum_i \frac{w^i}{\epsilon_1(p_T^i, y^i) \epsilon_2(p_T^i, y^i)}$. Here w^i is the signal $sPlot$ weight [88] used to remove the contribution of background and is obtained from the fit to the invariant-mass distribution, and $\epsilon_{1,2}(p_T^i, y^i)$ is the efficiency for the first and second hadron in the i^{th} candidate pair in data. The signal yield is then corrected for the charm-from- b contamination, which is estimated to be less than 1% for open charm pairs and $(4 \pm 2)\%$ ($(3.0 \pm 1.5)\%$) for $J/\psi D$ pairs in p Pb ($Pb p$) data.

Several sources of systematic uncertainties are investigated. The variation of the signal yield is studied with fits to the invariant-mass distribution using a different signal

or background model. A maximum relative variation of 2% is obtained on the signal yield. The dominant systematic uncertainty arises from the limited control sample size to determine the track finding efficiency, which is on average about 5% (10%) per track in $p\text{Pb}$ ($\text{Pb}p$) data. An uncertainty of 2% per hadron track is introduced to account for the loss of particles due to interactions with the detector material. Due to the small sample size and the choice of (p, η) binning for each track, the PID efficiencies obtained from control samples introduce an uncertainty of less than 1% on the total efficiency of each charm hadron. Other contributions include the uncertainty on the total efficiency due to the size of the simulation sample, the uncertainty on the charm decay branching fractions, the uncertainty on the luminosity measurements and on the charm-from- b fraction. These uncertainties are propagated to the cross-section measurements.

Total cross-sections are determined for all charm pairs. Results are detailed in the Supplemental Material. For LS open charm pairs, the measurements are in good agreement with theoretical calculations including both SPS and DPS production [42]. The $J/\psi D^0$ cross-section is found to be generally higher than SPS production, calculated using the weighted EPPS16 nPDF [89–92].

Prompt single charm cross-sections in $p\text{Pb}$ data were measured to be smaller than those of $\text{Pb}p$ data [76, 93], which is explained by modifications of the nPDF. The same effect would result in even stronger suppression of DPS production in $p\text{Pb}$ compared to $\text{Pb}p$ data due to the participation of two pairs of partons. For charm pairs, the cross-section ratio between $p\text{Pb}$ and $\text{Pb}p$ data, the forward-backward ratio (R_{FB}), is determined for $2.7 < |y(H_c)| < 3.7, p_{\text{T}}(H_c) > 2 \text{ GeV}/c$, to be $0.40 \pm 0.05 \pm 0.10$ ($0.61 \pm 0.04 \pm 0.12$) averaged over LS (OS) open charm pairs, and is $0.26 \pm 0.06 \pm 0.04$ for $J/\psi D$ pairs. Here and in the following, the first uncertainty is statistical and the second is systematic. The results indicate reduced production in $p\text{Pb}$ compared to $\text{Pb}p$ data for both LS and OS pairs. The R_{FB} of OS production is compatible with that of prompt D^0 mesons [76, 93], while that of LS production is smaller. The ratio between the R_{FB} of LS and OS production, $0.66 \pm 0.09 \pm 0.03$, is in good agreement with the R_{FB} of OS data and the R_{FB} of prompt D^0 production. The measurements favor the interpretation of LS production via DPS.

The LS over OS cross-section ratio, $R^{D_1 D_2} \equiv \sigma^{D_1 D_2} / \sigma^{D_1 \bar{D}_2}$, is determined for all studied $D_1 D_2$ pairs under the $p_{\text{T}}(D) > 2 \text{ GeV}/c$ requirement, giving an average value of $0.308 \pm 0.015 \pm 0.010$ and $0.391 \pm 0.019 \pm 0.025$ for $p\text{Pb}$ and $\text{Pb}p$ data respectively. The measurements agree with the calculations in Ref. [42] of $0.57_{-0.41}^{+0.16}$ ($p\text{Pb}$) and $0.52_{-0.38}^{+0.17}$ ($\text{Pb}p$), and are significantly larger than that in pp collisions where $R^{D^0 D^0} = 0.109 \pm 0.008$ [49], indicating an enhancement of LS pair production over OS pairs in $p\text{-Pb}$ collisions. The differential results as a function of $y(H_c)$ is shown in the Supplemental Material.

The correlations of kinematics between the two charm hadrons in a pair are investigated from the distributions of the two-charm invariant mass (m_{DD}) and their relative azimuthal angle $\Delta\phi$. The differential cross-section for each variable is normalized by the total cross-section, such that the largest systematic uncertainty, the one from the track finding efficiency, almost completely cancels. As examples, in Fig. 2, the m_{DD} distribution is shown for $D^0 D^0$ and $D^0 \bar{D}^0$ pairs without any requirement on $p_{\text{T}}(D)$. The difference between $D^0 D^0$ and $D^0 \bar{D}^0$ pairs is determined to be more than three (two) standard deviations in $p\text{Pb}$ ($\text{Pb}p$) data, studied using a χ^2 test. For both $D^0 D^0$ and $D^0 \bar{D}^0$ pairs, the m_{DD} distribution is compatible between $p\text{Pb}$ and $\text{Pb}p$ data. The $D^0 \bar{D}^0$ pair shows a similar m_{DD} distribution to that of the PYTHIA8 simulation, in which the fraction of inclusive charm production that contains more than one charm pair within the LHCb

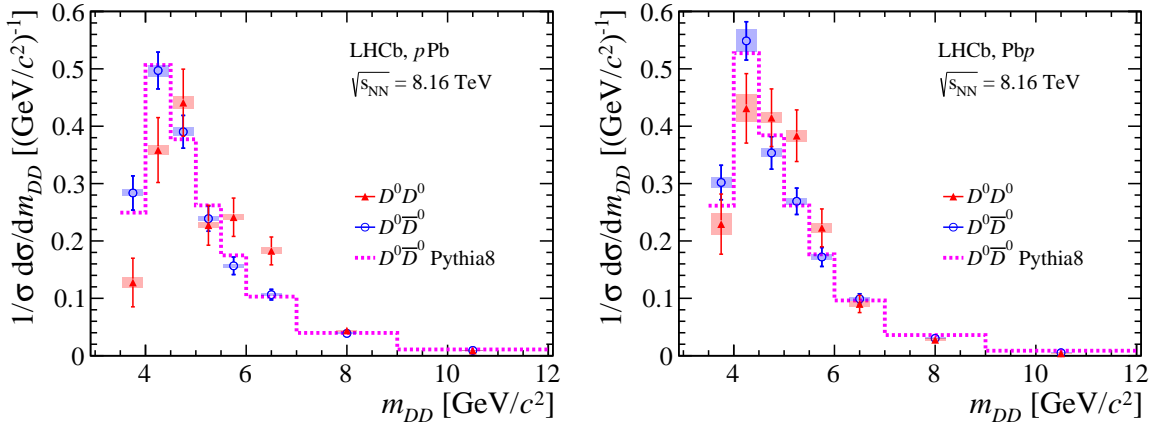


Figure 2: Two-charm hadron invariant-mass distribution of (red) $D^0 D^0$ and (blue) $D^0 \bar{D}^0$ pairs in (left) $p\text{Pb}$, (right) $\text{Pb}p$ data and (magenta dashed line) PYTHIA8 simulation. Vertical bars (filled box) are statistical (systematic) uncertainties.

acceptance is about 7%.

The $\Delta\phi$ distribution is shown in Fig. 3 for $D^0 D^0$ and $D^0 \bar{D}^0$ pairs with and without the requirement $p_T(D^0) > 2 \text{ GeV}/c$. Without this condition, the $\Delta\phi$ distribution is almost uniform for both LS and OS pairs, similar to that in PYTHIA8 simulation. However, with the $p_T(D^0) > 2 \text{ GeV}/c$ requirement, the $D^0 \bar{D}^0$ pair favors values $\Delta\phi \sim 0$, while that of $D^0 D^0$ pairs is still compatible with being flat, and both show inconsistency with the PYTHIA8 simulation. In general, the behaviour that m_{DD} distribution in $D^0 D^0$ pairs peaks at higher values compared to that of $D^0 \bar{D}^0$ pairs and the flat $D^0 D^0$ $\Delta\phi$ distribution are qualitatively consistent with a large DPS contribution in LS pair production. Distributions of the pair transverse momentum and the two-charm relative rapidity are found to be compatible in OS data, LS data and the PYTHIA8 simulation.

The effective cross-section $\sigma_{\text{eff}, p\text{Pb}}$ is calculated according to Eq. 1 using the $D^0 D^0$ and $J/\psi D^0$ cross-sections [6], assuming solely DPS production, where the prompt J/ψ and D^0 production are evaluated from LHCb measurements [75, 76]. The results are displayed in Table 1 with a typical value of order 1 b. The $\sigma_{\text{eff}, p\text{Pb}}$ measurement is about a factor of three smaller than the one obtained by the scaling the $\sigma_{\text{eff}, pp}$ result [78] by the Pb nucleus mass number 208, under the assumption that there is no nuclear modification for DPS production, which is shown in Table 1 as pp extrapolation. The result confirms the expectation that DPS production in $p\text{-Pb}$ collisions is enhanced by a factor of three [10, 37–42]. The $\sigma_{\text{eff}, p\text{Pb}}$ value measured using $J/\psi D^0$ production is smaller than that observed in $D^0 D^0$ production, as measured in pp data [78], which could be due

Table 1: The effective cross-section $\sigma_{\text{eff}, p\text{Pb}}$ (in b) measured using $J/\psi D^0$ and $D^0 D^0$ pair production in $p\text{-Pb}$ data and the extrapolated values from pp data [78].

Pairs	$-5 < y(H_c) < -2.5$	$1.5 < y(H_c) < 4$	pp extrapolation
$D^0 D^0$	$0.99 \pm 0.09 \pm 0.09$	$1.41 \pm 0.11 \pm 0.10$	4.3 ± 0.5
$J/\psi D^0$	$0.64 \pm 0.10 \pm 0.06$	$0.92 \pm 0.22 \pm 0.06$	3.1 ± 0.3

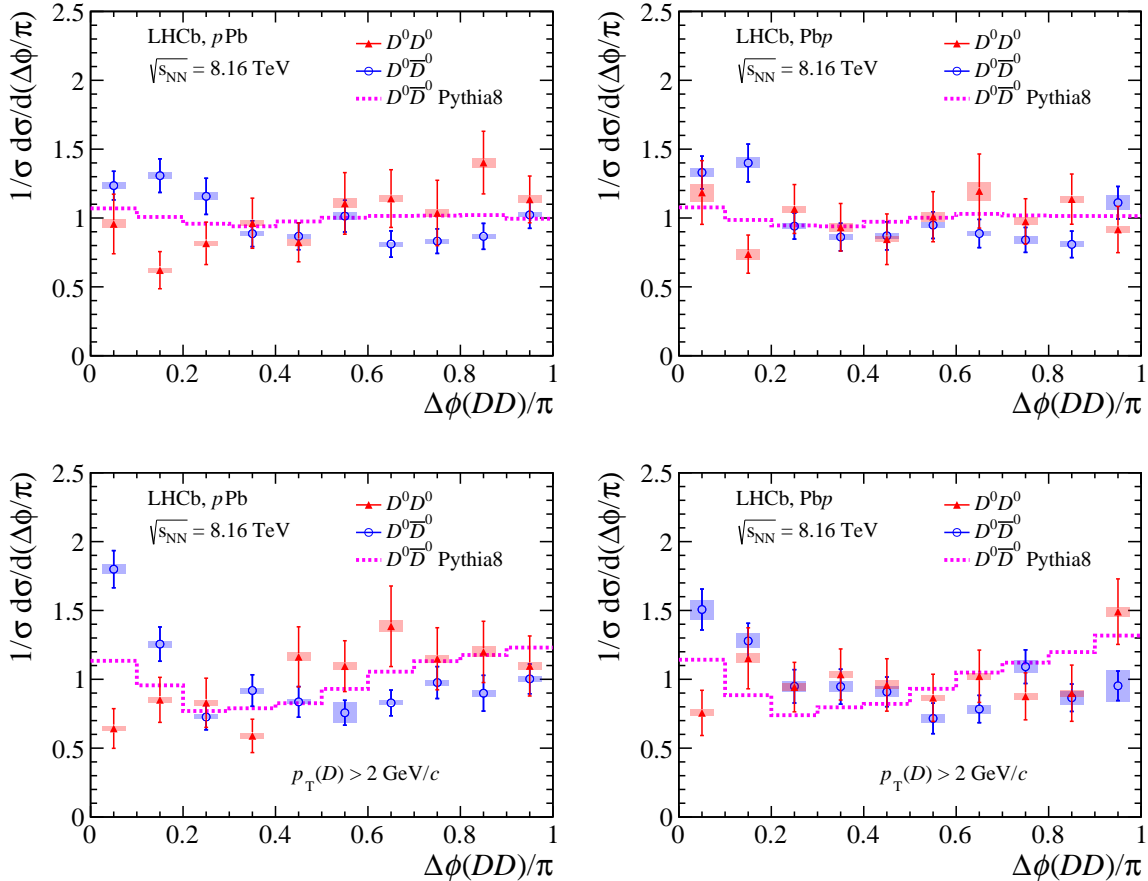


Figure 3: The $\Delta\phi$ distribution for (red) D^0D^0 and (blue) $D^0\bar{D}^0$ pairs in (left) $p\text{Pb}$, (right) Pbp data and the (magenta dashed line) PYTHIA8 simulation, (bottom) with and (top) without the $p_{\text{T}}(D^0) > 2 \text{ GeV}/c$ requirement. Vertical bars (filled box) are statistical (systematic) uncertainties.

to SPS contamination [94] or DPS enhancement in $J/\psi D^0$ production. The $p\text{Pb}$ data shows a higher $\sigma_{\text{eff}, p\text{Pb}}$ value compared to Pbp data, suggesting a different level of DPS enhancement when comparing $p\text{Pb}$ and Pbp data.

The nuclear modification factor, $R \equiv \frac{\sigma_{p\text{Pb}}}{208\sigma_{pp}}$, is measured for $J/\psi D^0$ and $D^0 D^0$ pairs with $R^{H_c H'_c} = R^{H_c} \times R^{H'_c} \times \frac{208\sigma_{\text{eff}, pp}}{\sigma_{\text{eff}, p\text{Pb}}}$, where $\sigma_{p\text{Pb}}$ and σ_{pp} are the cross-sections of charm pairs in $p\text{-Pb}$ and pp collisions, respectively. Assuming variations of R and $\sigma_{\text{eff}, pp}$ as a function of collision energy are small for p_{T} -integrated production, using measurements of $\sigma_{\text{eff}, pp}$ [49], $R^{J/\psi}$ [75] and R^{D^0} [93], $R^{D^0 D^0} = 1.3 \pm 0.2$ (4.2 ± 0.8) and $R^{J/\psi D^0} = 1.5 \pm 0.5$ (4.6 ± 1.3) for $p\text{Pb}$ (Pbp) data are obtained, where the uncertainties are the total. The results are about a factor of three larger compared to that of single J/ψ or D^0 hadron production [75, 93].

To summarise, the production of LS and OS open charm hadron pairs as well as $J/\psi D$ pairs are studied in $p\text{-Pb}$ collisions at $\sqrt{s_{\text{NN}}} = 8.16 \text{ TeV}$ using fully reconstructed decays. The cross-section ratio between LS and OS pairs is found to be a factor of three higher than that in pp data. The forward-backward ratio of OS pairs is compatible with

single charm production, while a smaller value is found for LS pairs. Distributions of the two-charm invariant mass and relative azimuthal angle show a difference between LS and OS pairs, and the LS pairs exhibit a flat relative azimuthal angle distribution independent of charm hadron p_T . The measured effective cross-sections of $J/\psi D^0$ and $D^0 D^0$ pairs are significantly different from values scaled from pp collisions assuming no nuclear modification. The effective cross-section and nuclear modification factor for $J/\psi D^0$ and $D^0 D^0$ are in general compatible with the expected enhancement factor of three for DPS production. The findings indicate the first direct observation of enhanced double parton scattering for charm production in p -Pb data. The $\sigma_{\text{eff}, p\text{Pb}}$ result is different between $p\text{Pb}$ and $\text{Pb}p$ data and between $J/\psi D^0$ and $D^0 D^0$ pairs may suggest additional effects not considered yet, which deserve further investigation using future LHCb data samples.

Acknowledgements

We would like to thank Hannu Paukkunen and Huasheng Shao for providing theoretical predictions and helpful discussions. We express our gratitude to our colleagues in the CERN accelerator departments for the excellent performance of the LHC. We thank the technical and administrative staff at the LHCb institutes. We acknowledge support from CERN and from the national agencies: CAPES, CNPq, FAPERJ and FINEP (Brazil); MOST and NSFC (China); CNRS/IN2P3 (France); BMBF, DFG and MPG (Germany); INFN (Italy); NWO (Netherlands); MNiSW and NCN (Poland); MEN/IFA (Romania); MSHE (Russia); MinECo (Spain); SNSF and SER (Switzerland); NASU (Ukraine); STFC (United Kingdom); DOE NP and NSF (USA). We acknowledge the computing resources that are provided by CERN, IN2P3 (France), KIT and DESY (Germany), INFN (Italy), SURF (Netherlands), PIC (Spain), GridPP (United Kingdom), RRCKI and Yandex LLC (Russia), CSCS (Switzerland), IFIN-HH (Romania), CBPF (Brazil), PL-GRID (Poland) and OSC (USA). We are indebted to the communities behind the multiple open-source software packages on which we depend. Individual groups or members have received support from AvH Foundation (Germany); EPLANET, Marie Skłodowska-Curie Actions and ERC (European Union); A*MIDEX, ANR, Labex P2IO and OCEVU, and Région Auvergne-Rhône-Alpes (France); Key Research Program of Frontier Sciences of CAS, CAS PIFI, and the Thousand Talents Program (China); RFBR, RSF and Yandex LLC (Russia); GVA, XuntaGal and GENCAT (Spain); the Royal Society and the Leverhulme Trust (United Kingdom).

Supplemental Material

Invariant mass distributions and fit projections

The invariant mass distributions and the fit projections are shown in Fig. 4 for $D^0 D^0$ pairs in Pbp data, and in Figs. 5 and 6 for $D^0 \bar{D}^0$ and $J/\psi D^0$ pairs in both $p\text{Pb}$ and $\text{Pb}p$ data.

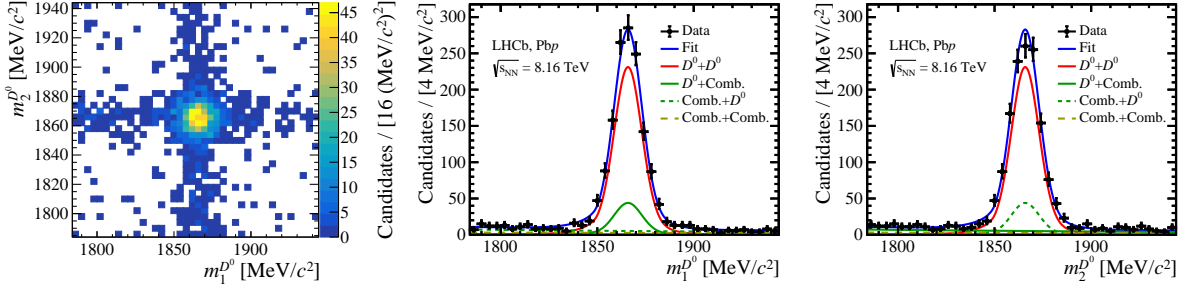


Figure 4: (Left) Two-dimensional invariant-mass distributions of (m_1, m_2) for $D^0 D^0$ pairs and the projections on (middle) m_1 and (right) m_2 with the fit results superimposed. Shown in the projection plots are (points with error bars) Pbp data, (solid blue) the total fit and the four fit components.

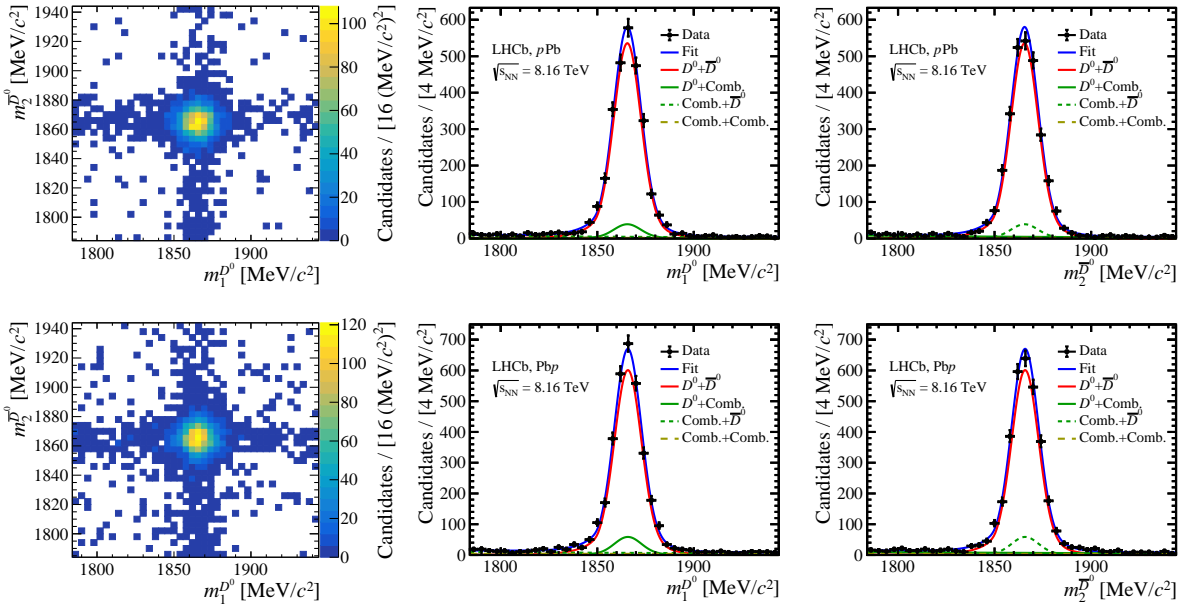


Figure 5: (Left) Two-dimensional invariant-mass distributions of (m_1, m_2) for $D^0 \bar{D}^0$ pairs and the projections on (middle) m_1 and (right) m_2 with the fit results superimposed. Shown in the projection plots are (points with error bars) data data, (solid blue) the total fit and the four fit components. The plots in the top (bottom) row correspond to $p\text{Pb}$ ($\text{Pb}p$) data.

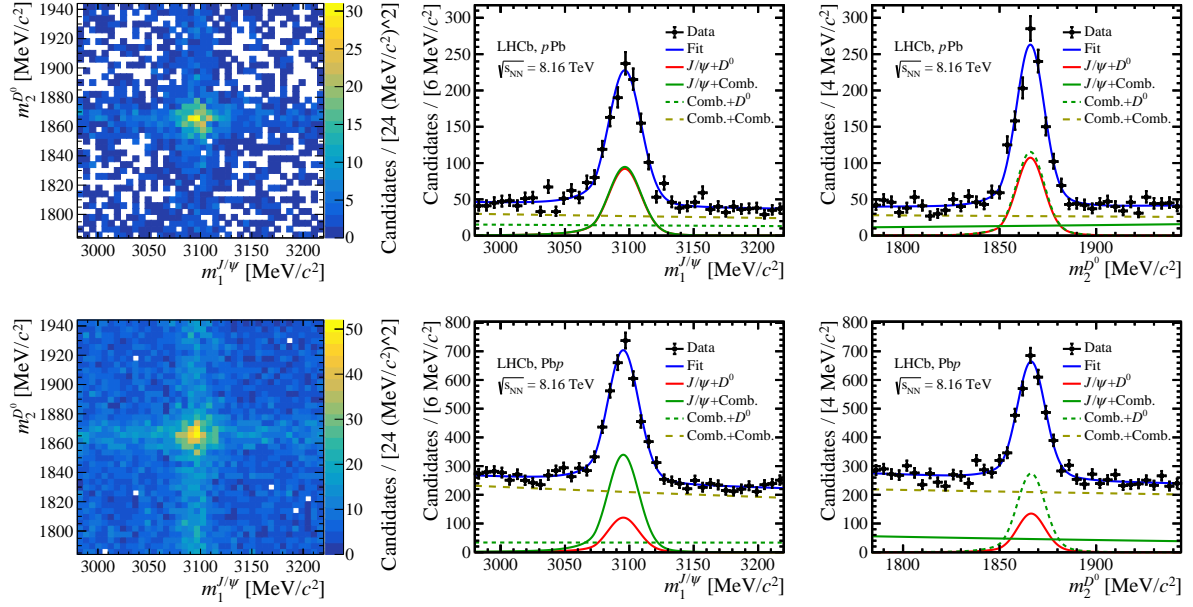


Figure 6: (Left) Two-dimensional invariant-mass distributions of $(m_1^{J/\psi}, m_2^{D^0})$ for $J/\psi D^0$ pairs and the projections on (middle) $m_1^{J/\psi}$ and (right) $m_2^{D^0}$ with the fit results superimposed. Shown in the projection plots are (points with error bars) data data, (solid blue) the total fit and the four fit components. The plots in the top (bottom) row correspond to $p\text{Pb}$ ($\text{Pb}p$) data.

Cross-sections and cross-section ratios

The total cross-sections measured in the reduced charm hadron rapidity ($y(H_c)$) range $1.7 < y(H_c) < 3.7$ ($-4.7 < y(H_c) < -2.7$) for $p\text{Pb}$ ($\text{Pb}p$) are shown in Table 2 under the requirement, $p_T > 0 \text{ GeV}/c$ for $J/\psi, D^0$ and $p_T > 2 \text{ GeV}/c$ for D^+, D_s^+ . The cross-section of $J/\psi D^0$ pair production is compared with the theoretical calculation of SPS production using the reweighted EPPS16 nuclear PDF [89–92]. Those with the additional requirement $p_T(D^0) > 2 \text{ GeV}/c$ are shown in Table 3, and those in full rapidity acceptance for $D^0 D^0, D^0 \bar{D}^0$ and $J/\psi D^0$ pairs are shown in Table 4.

In Table 5 and Fig. 7, the ratio between cross-sections of like-sign and opposite-sign pairs is shown in bins of charm hadron rapidity for $p_T(H_c) > 2 \text{ GeV}/c$.

Table 2: Total cross-sections of charm pair production (in mb) in $p\text{Pb}$ and $\text{Pb}p$ data for the p_T requirement on the charm hadron, $p_T > 0 \text{ GeV}/c$ for $J/\psi, D^0$ and $p_T > 2 \text{ GeV}/c$ for D^+, D_s^+ . The rapidity range is for each charm hadron in the pair. The first uncertainty is statistical and the second is systematic. The prediction of SPS $J/\psi D^0$ production calculated using the weighted EPPS16 nuclear PDF [89–92] is also listed for comparison, where the first uncertainty is from uncertainties of scales, feed-down contribution and model parameters, and the second due to nuclear PDF uncertainties.

Quantity	$1.7 < y(H_c) < 3.7$	$-4.7 < y(H_c) < -2.7$
$D^0 D^0$	$11.0 \pm 0.7 \pm 1.2$	$16.5 \pm 1.1 \pm 3.5$
$D^0 \bar{D}^0$	$34.1 \pm 1.2 \pm 3.6$	$35.1 \pm 1.3 \pm 5.9$
$D^0 D^+$	$4.0 \pm 0.3 \pm 0.6$	$5.3 \pm 0.4 \pm 1.7$
$D^0 D^-$	$12.7 \pm 0.4 \pm 1.7$	$11.6 \pm 0.4 \pm 2.8$
$D^0 D_s^+$	$2.1 \pm 0.6 \pm 0.3$	$3.6 \pm 0.7 \pm 1.2$
$D^0 D_s^-$	$5.4 \pm 0.6 \pm 0.8$	$7.1 \pm 1.0 \pm 1.8$
$D^+ D^+$	$0.46 \pm 0.05 \pm 0.09$	$0.53 \pm 0.08 \pm 0.24$
$D^+ D^-$	$1.38 \pm 0.07 \pm 0.22$	$1.26 \pm 0.08 \pm 0.42$
$D^+ D_s^-$	$1.43 \pm 0.21 \pm 0.25$	$1.32 \pm 0.20 \pm 0.44$
$D^+ D_s^+$	$0.32 \pm 0.12 \pm 0.05$	$0.80 \pm 0.27 \pm 0.40$
$J/\psi D^0$	$0.46 \pm 0.05 \pm 0.04$	$0.57 \pm 0.07 \pm 0.09$
$J/\psi D^+$	$0.08 \pm 0.01 \pm 0.01$	$0.10 \pm 0.01 \pm 0.02$
$J/\psi D^0$ SPS [89–92]	$0.051^{+0.467+0.009}_{-0.043-0.009}$	$0.055^{+0.426+0.004}_{-0.053-0.003}$

Table 3: Total production cross-sections (in mb) of open charm pairs involving the D^0 meson in $p\text{Pb}$ and $\text{Pb}p$ data with the $p_T(D^0) > 2 \text{ GeV}/c$ requirement. The rapidity range is for each charm hadron in the pair. The first uncertainty is statistical and the second is systematic. Predictions for the $D^0 D^0$ and $D^0 \bar{D}^0$ cross-sections from Ref. [42] are given in the last two rows of the Table.

Pairs	$1.7 < y(H_c) < 3.7$	$-4.7 < y(H_c) < -2.7$
$D^0 D^0$	$2.36 \pm 0.16 \pm 0.24$	$2.28 \pm 0.15 \pm 0.33$
$D^0 \bar{D}^0$	$7.36 \pm 0.28 \pm 0.71$	$6.01 \pm 0.24 \pm 0.81$
$D^0 D^+$	$1.83 \pm 0.12 \pm 0.26$	$1.97 \pm 0.13 \pm 0.54$
$D^0 D^-$	$6.27 \pm 0.19 \pm 0.82$	$5.06 \pm 0.17 \pm 1.07$
$D^0 D_s^+$	$0.84 \pm 0.19 \pm 0.13$	$1.46 \pm 0.50 \pm 0.38$
$D^0 D_s^-$	$3.03 \pm 0.34 \pm 0.45$	$2.38 \pm 0.29 \pm 0.50$
$J/\psi D^0$	$0.21 \pm 0.02 \pm 0.02$	$0.22 \pm 0.02 \pm 0.03$
$D^0 D^0$ [42]	$3.62^{+5.92}_{-3.37}$	$2.93^{+4.72}_{-2.69}$
$D^0 \bar{D}^0$ [42]	$6.34^{+8.66}_{-4.79}$	$5.59^{+7.41}_{-3.79}$

Table 4: Total cross-sections (in mb) in $p\text{Pb}$ and $\text{Pb}p$ data for full rapidity acceptance without any $p_{\text{T}}(H_c)$ requirement. The first uncertainty is statistical and the second is systematic.

Pairs	$1.5 < y(H_c) < 4$	$-5 < y(H_c) < -2.5$
$D^0\bar{D}^0$	$14.72 \pm 1.10 \pm 2.25$	$24.05 \pm 2.12 \pm 5.19$
$D^0\bar{D}^0$	$45.99 \pm 2.09 \pm 5.04$	$52.05 \pm 2.40 \pm 8.91$
$J/\psi D^0$	$0.51 \pm 0.12 \pm 0.05$	$0.82 \pm 0.13 \pm 0.14$

Table 5: Ratios of differential cross-sections in bins of charm hadron rapidity for charm $p_{\text{T}}(H_c) > 2 \text{ GeV}/c$. The average over all the pairs in each rapidity interval is also presented.

Pairs	$-4.7 < y(H_c) < -3.7$	$-3.7 < y(H_c) < -2.7$	$1.7 < y(H_c) < 2.7$	$2.7 < y(H_c) < 3.7$
$D^0\bar{D}^0/D^0\bar{D}^0$	$0.286 \pm 0.067 \pm 0.011$	$0.363 \pm 0.040 \pm 0.009$	$0.305 \pm 0.041 \pm 0.009$	$0.335 \pm 0.060 \pm 0.012$
D^0D^+/D^0D^-	$0.239 \pm 0.046 \pm 0.017$	$0.387 \pm 0.047 \pm 0.026$	$0.259 \pm 0.045 \pm 0.010$	$0.256 \pm 0.037 \pm 0.009$
D^+D^+/D^+D^-	$0.300 \pm 0.090 \pm 0.037$	$0.518 \pm 0.157 \pm 0.079$	$0.332 \pm 0.070 \pm 0.018$	$0.266 \pm 0.061 \pm 0.012$
$D^0D_s^+/D^0D_s^-$	$0.321 \pm 0.260 \pm 0.043$	$0.504 \pm 0.172 \pm 0.028$	$0.201 \pm 0.096 \pm 0.006$	$0.303 \pm 0.139 \pm 0.014$
$D^+D_s^+/D^+D_s^-$	$0.291 \pm 0.590 \pm 0.080$	$0.582 \pm 0.340 \pm 0.113$	$0.143 \pm 0.116 \pm 0.009$	$0.234 \pm 0.113 \pm 0.013$
Average	$0.262 \pm 0.035 \pm 0.019$	$0.384 \pm 0.029 \pm 0.019$	$0.278 \pm 0.026 \pm 0.010$	$0.274 \pm 0.027 \pm 0.011$

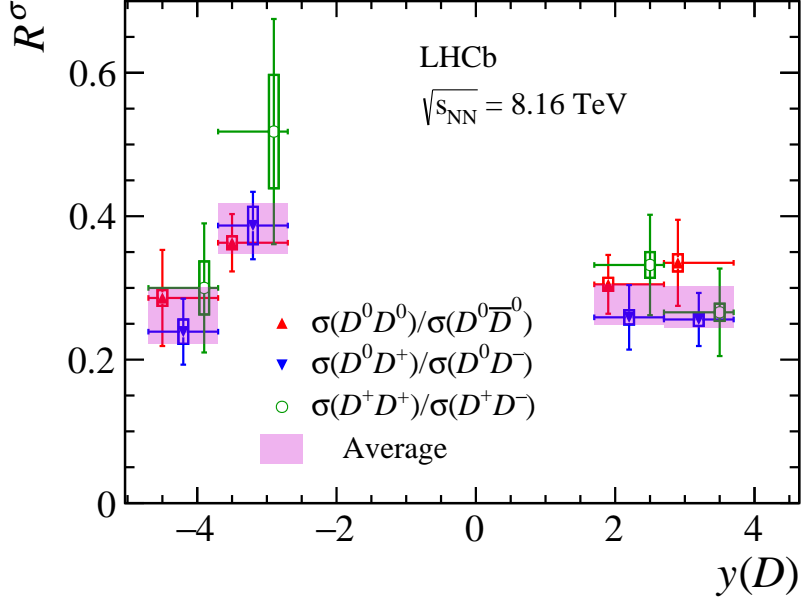


Figure 7: Ratios of differential cross-sections in bins of charm hadron rapidity under the $p_{\text{T}}(D) > 2 \text{ GeV}/c$ requirement. The average over all the pairs listed in Table 5 for each rapidity interval is also presented. The boxes (bars) correspond to systematic (statistical) uncertainties. Points are shifted horizontally to improve visibility.

References

- [1] H. Abramowicz *et al.*, *Summary of the workshop on multi-parton interactions (MPI@LHC 2012)*, arXiv:1306.5413.
- [2] ALICE collaboration, B. Abelev *et al.*, *J/ψ production as a function of charged particle multiplicity in pp collisions at $\sqrt{s} = 7$ TeV*, Phys. Lett. **B712** (2012) 165, arXiv:1202.2816.
- [3] ALICE collaboration, S. Acharya *et al.*, *Measurement of electrons from heavy-flavour hadron decays as a function of multiplicity in p -Pb collisions at $\sqrt{s_{NN}} = 5.02$ TeV*, JHEP **02** (2020) 077, arXiv:1910.14399.
- [4] P. Bartalini and J. R. Gaunt, *Multiple parton interactions at the LHC*, Adv. Ser. Direct. High Energy Phys. **29** (2018) 1.
- [5] CDF collaboration, F. Abe *et al.*, *Double parton scattering in $\bar{p}p$ collisions at $\sqrt{s} = 1.8$ TeV*, Phys. Rev. **D56** (1997) 3811.
- [6] M. H. Seymour and A. Siodmok, *Extracting $\sigma_{\text{effective}}$ from the LHCb double-charm measurement*, arXiv:1308.6749.
- [7] J. R. Gaunt and W. J. Stirling, *Double parton distributions incorporating perturbative QCD evolution and momentum and quark number sum rules*, JHEP **03** (2010) 005, arXiv:0910.4347.
- [8] J. R. Gaunt, C.-H. Kom, A. Kulesza, and W. J. Stirling, *Same-sign W pair production as a probe of double parton scattering at the LHC*, Eur. Phys. J. **C69** (2010) 53, arXiv:1003.3953.
- [9] C. H. Kom, A. Kulesza, and W. J. Stirling, *Pair production of J/ψ as a probe of double parton scattering at LHCb*, Phys. Rev. Lett. **107** (2011) 082002, arXiv:1105.4186.
- [10] M. Łuszczak, R. Maciuła, and A. Szczurek, *Production of two $c\bar{c}$ pairs in double-parton scattering*, Phys. Rev. **D85** (2012) 094034, arXiv:1111.3255.
- [11] S. P. Baranov, A. M. Snigirev, and N. P. Zotov, *Double heavy meson production through double parton scattering in hadronic collisions*, Phys. Lett. **B705** (2011) 116, arXiv:1105.6276.
- [12] P. Bartalini *et al.*, *Multi-parton interactions at the LHC*, 2011, arXiv:1111.0469.
- [13] J.-P. Lansberg, H.-S. Shao, N. Yamanaka, and Y.-J. Zhang, *Prompt J/ψ -pair production at the LHC: Impact of loop-induced contributions and of the colour-octet mechanism*, Eur. Phys. J. **C79** (2019) 1006, arXiv:1906.10049.
- [14] M. Alvioli, M. Azarkin, B. Blok, and M. Strikman, *Revealing minijet dynamics via centrality dependence of double parton interactions in proton-nucleus collisions*, Eur. Phys. J. **C79** (2019) 482, arXiv:1901.11266.
- [15] M. G. Ryskin and A. M. Snigirev, *A fresh look at double parton scattering*, Phys. Rev. **D83** (2011) 114047, arXiv:1103.3495.

- [16] D. Treleani, *Double parton scattering, diffraction and effective cross section*, Phys. Rev. **D76** (2007) 076006, arXiv:0708.2603.
- [17] G. Calucci and D. Treleani, *Proton structure in transverse space and the effective cross-section*, Phys. Rev. **D60** (1999) 054023, arXiv:hep-ph/9902479.
- [18] R. Vogt, *Heavy flavor azimuthal correlations in cold nuclear matter*, Phys. Rev. **C98** (2018) 034907, arXiv:1806.01904.
- [19] R. Vogt, *$b\bar{b}$ kinematic correlations in cold nuclear matter*, Phys. Rev. **C101** (2020) 024910, arXiv:1908.05320.
- [20] C. Marquet, C. Roiesnel, and P. Taels, *Linearly polarized small- x gluons in forward heavy-quark pair production*, Phys. Rev. **D97** (2018) 014004, arXiv:1710.05698.
- [21] J. L. Albacete, G. Giacalone, C. Marquet, and M. Matas, *Forward dihadron back-to-back correlations in pA collisions*, Phys. Rev. **D99** (2019) 014002, arXiv:1805.05711.
- [22] LHCb collaboration, *LHCb measurement projections in proton-lead collisions during Run 3 and 4*, LHCb-CONF-2018-005, 2018.
- [23] S. Shi, X. Dong, and M. Mustafa, *A study of charm quark correlations in ultra-relativistic $p + p$ collisions with PYTHIA*, arXiv:1507.00614.
- [24] S. Cao, G.-Y. Qin, and S. A. Bass, *Modeling of heavy-flavor pair correlations in Au-Au collisions at 200A GeV at the BNL Relativistic Heavy Ion Collider*, Phys. Rev. **C92** (2015) 054909, arXiv:1505.01869.
- [25] X. Zhu *et al.*, *$DD\bar{D}$ correlations as a sensitive probe for thermalization in high-energy nuclear collisions*, Phys. Lett. **B647** (2007) 366, arXiv:hep-ph/0604178.
- [26] T. Lang, H. van Hees, J. Steinheimer, and M. Bleicher, *Dileptons from correlated D - and \bar{D} -meson decays in the invariant mass range of the QGP thermal radiation using the UrQMD hybrid model*, arXiv:1305.7377.
- [27] H. He, Y. Liu, and P. Zhuang, *Ω_{ccc} production in high energy nuclear collisions*, Phys. Lett. **B746** (2015) 59, arXiv:1409.1009.
- [28] R. J. Fries, B. Müller, C. Nonaka, and S. A. Bass, *Hadronization in heavy ion collisions: Recombination and fragmentation of partons*, Phys. Rev. Lett. **90** (2003) 202303, arXiv:nucl-th/0301087.
- [29] R. J. Fries, B. Müller, C. Nonaka, and S. A. Bass, *Hadron production in heavy ion collisions: Fragmentation and recombination from a dense parton phase*, Phys. Rev. **C68** (2003) 044902, arXiv:nucl-th/0306027.
- [30] J.-P. Blaizot, D. De Boni, P. Faccioli, and G. Garberoglio, *Heavy quark bound states in a quark-gluon plasma: Dissociation and recombination*, Nucl. Phys. **A946** (2016) 49, arXiv:1503.03857.
- [31] S. Cho and S. H. Lee, *Production of multicharmed hadrons by recombination in heavy ion collisions*, Phys. Rev. **C101** (2020) 024902, arXiv:1907.12786.

- [32] R. L. Thews, M. Schroedter, and J. Rafelski, *Enhanced J/ψ production in deconfined quark matter*, Phys. Rev. **C63** (2001) 054905, arXiv:hep-ph/0007323.
- [33] A. Andronic, P. Braun-Munzinger, K. Redlich, and J. Stachel, *Statistical hadronization of charm in heavy ion collisions at SPS, RHIC and LHC*, Phys. Lett. **B571** (2003) 36, arXiv:nucl-th/0303036.
- [34] V. Greco, C. M. Ko, and R. Rapp, *Quark coalescence for charmed mesons in ultrarelativistic heavy ion collisions*, Phys. Lett. **B595** (2004) 202, arXiv:nucl-th/0312100.
- [35] ALICE collaboration, B. Abelev *et al.*, *J/ψ suppression at forward rapidity in Pb-Pb collisions at $\sqrt{s_{NN}} = 2.76$ TeV*, Phys. Rev. Lett. **109** (2012) 072301, arXiv:1202.1383.
- [36] X. Yao and B. Müller, *Quarkonium inside the quark-gluon plasma: Diffusion, dissociation, recombination, and energy loss*, Phys. Rev. **D100** (2019) 014008, arXiv:1811.09644.
- [37] M. Strikman and D. Treleani, *Measuring double parton distributions in nucleons at proton nucleus colliders*, Phys. Rev. Lett. **88** (2002) 031801, arXiv:hep-ph/0111468.
- [38] D. d’Enterria and A. M. Snigirev, *Same-sign WW production in proton-nucleus collisions at the LHC as a signal for double parton scattering*, Phys. Lett. **B718** (2013) 1395, arXiv:1211.0197.
- [39] S. Salvini, D. Treleani, and G. Calucci, *Double parton scatterings in high-energy proton-nucleus collisions and partonic correlations*, Phys. Rev. **D89** (2014) 016020, arXiv:1309.6201.
- [40] E. R. Cazaroto, V. P. Gonçalves, and F. S. Navarra, *Heavy quark production in pA collisions: the double parton scattering contribution*, Mod. Phys. Lett. **A33** (2018) 1850141, arXiv:1607.04023.
- [41] D. d’Enterria and A. Snigirev, *Double, triple, and n-parton scatterings in high-energy proton and nuclear collisions*, Adv. Ser. Direct. High Energy Phys. **29** (2018) 159, arXiv:1708.07519.
- [42] I. Helenius and H. Paukkunen, *Double D-meson production in proton-proton and proton-lead collisions at the LHC*, Phys. Lett. **B800** (2020) 135084, arXiv:1906.06971.
- [43] B. Blok and F. A. Ceccopieri, *Double parton scattering in pA collisions at the LHC revisited*, Eur. Phys. J. **C80** (2020) 278, arXiv:1912.02508.
- [44] H.-S. Shao, *Probing impact-parameter dependent nuclear parton densities from double parton scatterings in heavy-ion collisions*, Phys. Rev. **D101** (2020) 054036, arXiv:2001.04256.
- [45] FOCUS collaboration, J. M. Link *et al.*, *Studies of correlations between D and \bar{D} mesons in high-energy photoproduction*, Phys. Lett. **B566** (2003) 51, arXiv:hep-ex/0305018.

- [46] E791 collaboration, E. M. Aitala *et al.*, *Correlations between D and \bar{D} mesons produced in 500 GeV/c π^- -nucleon interactions*, Eur. Phys. J. direct **1** (1999) 4, arXiv:hep-ex/9809029.
- [47] E687 collaboration, P. L. Frabetti *et al.*, *Studies of $D\bar{D}$ correlations in high-energy photoproduction*, Phys. Lett. **B308** (1993) 193.
- [48] ACCMOR collaboration, S. Barlag *et al.*, *Charmed pair correlations in π^- Cu interactions at 230 GeV/c.*, Phys. Lett. **B302** (1993) 112.
- [49] LHCb collaboration, R. Aaij *et al.*, *Observation of double charm production involving open charm in pp collisions at $\sqrt{s} = 7$ TeV*, JHEP **06** (2012) 141, Addendum ibid. **03** (2014) 108, arXiv:1205.0975.
- [50] PHENIX collaboration, C. Aidala *et al.*, *Correlations of $\mu\mu$, $e\mu$, and ee pairs in p+p collisions at $\sqrt{s} = 200$ GeV and implications for $c\bar{c}$ and $b\bar{b}$ production mechanisms*, Submitted to: Phys. Rev. Lett. (2018) arXiv:1805.04075.
- [51] UA1 collaboration, C. Albajar *et al.*, *Measurement of $b\bar{b}$ correlations at the CERN $p\bar{p}$ collider*, Z. Phys. **C61** (1994) 41.
- [52] CDF collaboration, F. Abe *et al.*, *Measurement of $b\bar{b}$ rapidity correlations in $p\bar{p}$ collisions at $\sqrt{s} = 1.8$ TeV*, Phys. Rev. **D61** (2000) 032001.
- [53] CDF collaboration, D. Acosta *et al.*, *Measurements of $b\bar{b}$ azimuthal production correlations in $p\bar{p}$ collisions at $\sqrt{s} = 1.8$ TeV*, Phys. Rev. **D71** (2005) 092001, arXiv:hep-ex/0412006.
- [54] CDF collaboration, T. Aaltonen *et al.*, *Measurement of correlated $b\bar{b}$ production in $p\bar{p}$ collisions at $\sqrt{s} = 1960$ GeV*, Phys. Rev. **D77** (2008) 072004, arXiv:0710.1895.
- [55] D0 collaboration, B. Abbott *et al.*, *The $b\bar{b}$ production cross section and angular correlations in $p\bar{p}$ collisions at $\sqrt{s} = 1.8$ TeV*, Phys. Lett. **B487** (2000) 264, arXiv:hep-ex/9905024.
- [56] LHCb collaboration, R. Aaij *et al.*, *Study of $b\bar{b}$ correlations in high energy proton-proton collisions*, JHEP **11** (2017) 030, arXiv:1708.05994.
- [57] CMS collaboration, V. Khachatryan *et al.*, *Measurement of $B\bar{B}$ Angular Correlations based on Secondary Vertex Reconstruction at $\sqrt{s} = 7$ TeV*, JHEP **03** (2011) 136, arXiv:1102.3194.
- [58] LHCb collaboration, R. Aaij *et al.*, *Observation of J/ψ -pair production in pp collisions at $\sqrt{s} = 7$ TeV*, Phys. Lett. **B707** (2012) 52, arXiv:1109.0963.
- [59] LHCb collaboration, R. Aaij *et al.*, *Measurement of the J/ψ pair production cross-section in pp collisions at $\sqrt{s} = 13$ TeV*, JHEP **06** (2017) 047, Erratum ibid. **10** (2017) 068, arXiv:1612.07451.
- [60] LHCb collaboration, R. Aaij *et al.*, *Production of associated Υ and open charm hadrons in pp collisions at $\sqrt{s} = 7$ and 8 TeV via double parton scattering*, JHEP **07** (2016) 052, arXiv:1510.05949.

- [61] CMS collaboration, V. Khachatryan *et al.*, *Observation of $\Upsilon(1S)$ pair production in proton-proton collisions at $\sqrt{s} = 8$ TeV*, JHEP **05** (2017) 013, arXiv:1610.07095.
- [62] CMS collaboration, V. Khachatryan *et al.*, *Measurement of prompt J/ψ pair production in pp collisions at $\sqrt{s} = 7$ TeV*, JHEP **09** (2014) 094, arXiv:1406.0484.
- [63] D0 collaboration, V. M. Abazov *et al.*, *Evidence for simultaneous production of J/ψ and Υ mesons*, Phys. Rev. Lett. **116** (2016) 082002, arXiv:1511.02428.
- [64] CDF collaboration, F. Abe *et al.*, *Study of four jet events and evidence for double parton interactions in $p\bar{p}$ collisions at $\sqrt{s} = 1.8$ TeV*, Phys. Rev. **D47** (1993) 4857.
- [65] ATLAS collaboration, M. Aaboud *et al.*, *Study of hard double-parton scattering in four-jet events in pp collisions at $\sqrt{s} = 7$ TeV with the ATLAS experiment*, JHEP **11** (2016) 110, arXiv:1608.01857.
- [66] CDF collaboration, F. Abe *et al.*, *Measurement of double parton scattering in $p\bar{p}$ collisions at $\sqrt{s} = 1.8$ TeV*, Phys. Rev. Lett. **79** (1997) 584.
- [67] ATLAS collaboration, M. Aaboud *et al.*, *Measurement of the prompt J/ψ pair production cross-section in pp collisions at $\sqrt{s} = 8$ TeV with the ATLAS detector*, Eur. Phys. J. **C77** (2017) 76, arXiv:1612.02950.
- [68] J.-P. Lansberg, H.-S. Shao, and N. Yamanaka, *Indication for double parton scatterings in $W +$ prompt J/ψ production at the LHC*, Phys. Lett. **B781** (2018) 485, arXiv:1707.04350.
- [69] J.-P. Lansberg and H.-S. Shao, *J/ψ -pair production at large momenta: Indications for double parton scatterings and large α_s^5 contributions*, Phys. Lett. **B751** (2015) 479, arXiv:1410.8822.
- [70] LHCb collaboration, A. A. Alves Jr. *et al.*, *The LHCb detector at the LHC*, JINST **3** (2008) S08005.
- [71] LHCb collaboration, R. Aaij *et al.*, *LHCb detector performance*, Int. J. Mod. Phys. **A30** (2015) 1530022, arXiv:1412.6352.
- [72] R. Aaij *et al.*, *Selection and processing of calibration samples to measure the particle identification performance of the LHCb experiment in Run 2*, Eur. Phys. J. Tech. Instr. **6** (2018) 1, arXiv:1803.00824.
- [73] F. Archilli *et al.*, *Performance of the muon identification at LHCb*, JINST **8** (2013) P10020, arXiv:1306.0249.
- [74] Particle Data Group, M. Tanabashi *et al.*, *Review of particle physics*, Phys. Rev. **D98** (2018) 030001, and 2019 update.
- [75] LHCb collaboration, R. Aaij *et al.*, *Prompt and nonprompt J/ψ production and nuclear modification in pPb collisions at $\sqrt{s_{NN}} = 8.16$ TeV*, Phys. Lett. **B774** (2017) 159, arXiv:1706.07122.

- [76] LHCb collaboration, R. Aaij *et al.*, *Study of prompt D^0 meson production in pPb at $\sqrt{s_{NN}} = 8.16$ TeV at LHCb*, LHCb-CONF-2019-004, 2019.
- [77] CLEO collaboration, J. P. Alexander *et al.*, *Absolute measurement of hadronic branching fractions of the D_s^+ meson*, Phys. Rev. Lett. **100** (2008) 161804, arXiv:0801.0680.
- [78] LHCb collaboration, R. Aaij *et al.*, *Measurements of prompt charm production cross-sections in pp collisions at $\sqrt{s} = 5$ TeV*, JHEP **06** (2017) 147, arXiv:1610.02230.
- [79] T. Skwarnicki, *A study of the radiative cascade transitions between the Upsilon-prime and Upsilon resonances*, PhD thesis, Institute of Nuclear Physics, Krakow, 1986, DESY-F31-86-02.
- [80] LHCb collaboration, R. Aaij *et al.*, *Measurement of B^+ , B^0 and A_b^0 production in pPb collisions at $\sqrt{s_{NN}} = 8.16$ TeV*, Phys. Rev. **D99** (2019) 052011, arXiv:1902.05599.
- [81] T. Pierog *et al.*, *EPOS LHC: Test of collective hadronization with data measured at the CERN Large Hadron Collider*, Phys. Rev. **C92** (2015) 034906, arXiv:1306.0121.
- [82] T. Sjöstrand, S. Mrenna, and P. Skands, *A brief introduction to PYTHIA 8.1*, Comput. Phys. Commun. **178** (2008) 852, arXiv:0710.3820.
- [83] T. Sjöstrand, S. Mrenna, and P. Skands, *PYTHIA 6.4 physics and manual*, JHEP **05** (2006) 026, arXiv:hep-ph/0603175.
- [84] D. J. Lange, *The EvtGen particle decay simulation package*, Nucl. Instrum. Meth. **A462** (2001) 152.
- [85] Geant4 collaboration, J. Allison *et al.*, *Geant4 developments and applications*, IEEE Trans. Nucl. Sci. **53** (2006) 270; Geant4 collaboration, S. Agostinelli *et al.*, *Geant4: A simulation toolkit*, Nucl. Instrum. Meth. **A506** (2003) 250.
- [86] M. Clemencic *et al.*, *The LHCb simulation application, Gauss: Design, evolution and experience*, J. Phys. Conf. Ser. **331** (2011) 032023.
- [87] LHCb collaboration, R. Aaij *et al.*, *Measurement of the track reconstruction efficiency at LHCb*, JINST **10** (2015) P02007, arXiv:1408.1251.
- [88] M. Pivk and F. R. Le Diberder, *sPlot: A statistical tool to unfold data distributions*, Nucl. Instrum. Meth. **A555** (2005) 356, arXiv:physics/0402083.
- [89] H.-S. Shao, *HELAC-Onia 2.0: An upgraded matrix-element and event generator for heavy quarkonium physics*, Comput. Phys. Commun. **198** (2016) 238, arXiv:1507.03435.
- [90] H.-S. Shao, *HELAC-Onia: An automatic matrix element generator for heavy quarkonium physics*, Comput. Phys. Commun. **184** (2013) 2562, arXiv:1212.5293.
- [91] A. Kusina, J.-P. Lansberg, I. Schienbein, and H.-S. Shao, *Gluon shadowing in heavy-flavor production at the LHC*, Phys. Rev. Lett. **121** (2018) 052004, arXiv:1712.07024.

- [92] K. J. Eskola, P. Paakkinen, H. Paukkunen, and C. A. Salgado, *EPPS16: Nuclear parton distributions with LHC data*, Eur. Phys. J. **C77** (2017) 163, [arXiv:1612.05741](#).
- [93] LHCb collaboration, R. Aaij *et al.*, *Study of prompt D^0 meson production in pPb collisions at $\sqrt{s_{NN}}=5$ TeV*, JHEP **10** (2017) 090, [arXiv:1707.02750](#).
- [94] H.-S. Shao, *J/ψ meson production in association with an open charm hadron at the LHC: a reappraisal*, [arXiv:2005.12967](#).

LHCb collaboration

R. Aaij³¹, C. Abellán Beteta⁴⁹, T. Ackernley⁵⁹, B. Adeva⁴⁵, M. Adinolfi⁵³, H. Afsharnia⁹, C.A. Aidala⁸², S. Aiola²⁵, Z. Ajaltouni⁹, S. Akar⁶⁴, J. Albrecht¹⁴, F. Alessio⁴⁷, M. Alexander⁵⁸, A. Alfonso Alberio⁴⁴, Z. Aliouche⁶¹, G. Alkhazov³⁷, P. Alvarez Cartelle⁴⁷, A.A. Alves Jr⁴⁵, S. Amato², Y. Amhis¹¹, L. An²¹, L. Anderlini²¹, G. Andreassi⁴⁸, A. Andreianov³⁷, M. Andreotti²⁰, F. Archilli¹⁶, A. Artamonov⁴³, M. Artuso⁶⁷, K. Arzymatov⁴¹, E. Aslanides¹⁰, M. Atzeni⁴⁹, B. Audurier¹¹, S. Bachmann¹⁶, M. Bachmayer⁴⁸, J.J. Back⁵⁵, S. Baker⁶⁰, P. Baladron Rodriguez⁴⁵, V. Balagura^{11,b}, W. Baldini²⁰, J. Baptista Leite¹, R.J. Barlow⁶¹, S. Barsuk¹¹, W. Barter⁶⁰, M. Bartolini^{23,47,h}, F. Baryshnikov⁷⁹, J.M. Basels¹³, G. Bassi²⁸, V. Batozskaya³⁵, B. Batsukh⁶⁷, A. Battig¹⁴, A. Bay⁴⁸, M. Becker¹⁴, F. Bedeschi²⁸, I. Bediaga¹, A. Beiter⁶⁷, V. Belavin⁴¹, S. Belin²⁶, V. Bellee⁴⁸, K. Belous⁴³, I. Belyaev³⁸, G. Bencivenni²², E. Ben-Haim¹², A. Berezhnoy³⁹, R. Bernet⁴⁹, D. Berninghoff¹⁶, H.C. Bernstein⁶⁷, C. Bertella⁴⁷, E. Bertholet¹², A. Bertolin²⁷, C. Betancourt⁴⁹, F. Betti^{19,e}, M.O. Bettler⁵⁴, Ia. Bezshyiko⁴⁹, S. Bhasin⁵³, J. Bhom³³, L. Bian⁷², M.S. Bieker¹⁴, S. Bifani⁵², P. Billoir¹², M. Birch⁶⁰, F.C.R. Bishop⁵⁴, A. Bizzeti^{21,t}, M. Bjørn⁶², M.P. Blago⁴⁷, T. Blake⁵⁵, F. Blanc⁴⁸, S. Blusk⁶⁷, D. Bobulska⁵⁸, V. Bocci³⁰, J.A. Boelhauve¹⁴, O. Boente Garcia⁴⁵, T. Boettcher⁶³, A. Boldyrev⁸⁰, A. Bondar^{42,w}, N. Bondar^{37,47}, S. Borghi⁶¹, M. Borisyak⁴¹, M. Borsato¹⁶, J.T. Borsuk³³, S.A. Bouchiba⁴⁸, T.J.V. Bowcock⁵⁹, A. Boyer⁴⁷, C. Bozzi²⁰, M.J. Bradley⁶⁰, S. Braun⁶⁵, A. Brea Rodriguez⁴⁵, M. Brodski⁴⁷, J. Brodzicka³³, A. Brossa Gonzalo⁵⁵, D. Brundu²⁶, E. Buchanan⁵³, A. Buonaura⁴⁹, C. Burr⁴⁷, A. Bursche²⁶, A. Butkevich⁴⁰, J.S. Butter³¹, J. Buytaert⁴⁷, W. Byczynski⁴⁷, S. Cadeddu²⁶, H. Cai⁷², R. Calabrese^{20,g}, L. Calero Diaz²², S. Cali²², R. Calladine⁵², M. Calvi^{24,i}, M. Calvo Gomez^{44,l}, P. Camargo Magalhaes⁵³, A. Camboni⁴⁴, P. Campana²², D.H. Campora Perez⁴⁷, A.F. Campoverde Quezada⁵, S. Capelli^{24,i}, L. Capriotti^{19,e}, A. Carbone^{19,e}, G. Carboni²⁹, R. Cardinale^{23,h}, A. Cardini²⁶, I. Carli⁶, P. Carniti^{24,i}, K. Carvalho Akiba³¹, A. Casais Vidal⁴⁵, G. Casse⁵⁹, M. Cattaneo⁴⁷, G. Cavallero⁴⁷, S. Celani⁴⁸, R. Cenci²⁸, J. Cerasoli¹⁰, A.J. Chadwick⁵⁹, M.G. Chapman⁵³, M. Charles¹², Ph. Charpentier⁴⁷, G. Chatzikonstantinidis⁵², M. Chefdeville⁸, C. Chen³, S. Chen²⁶, A. Chernov³³, S.-G. Chitic⁴⁷, V. Chobanova⁴⁵, S. Cholak⁴⁸, M. Chruszcz³³, A. Chubykin³⁷, V. Chulikov³⁷, P. Ciambrone²², M.F. Cicala⁵⁵, X. Cid Vidal⁴⁵, G. Ciezarek⁴⁷, F. Cindolo¹⁹, P.E.L. Clarke⁵⁷, M. Clemencic⁴⁷, H.V. Cliff⁵⁴, J. Closier⁴⁷, J.L. Cobbledick⁶¹, V. Coco⁴⁷, J.A.B. Coelho¹¹, J. Cogan¹⁰, E. Cogneras⁹, L. Cojocariu³⁶, P. Collins⁴⁷, T. Colombo⁴⁷, A. Contu²⁶, N. Cooke⁵², G. Coombs⁵⁸, S. Coquereau⁴⁴, G. Corti⁴⁷, C.M. Costa Sobral⁵⁵, B. Couturier⁴⁷, D.C. Craik⁶³, J. Crkovská⁶⁶, M. Cruz Torres^{1,y}, R. Currie⁵⁷, C.L. Da Silva⁶⁶, E. Dall’Occo¹⁴, J. Dalseno⁴⁵, C. D’Ambrosio⁴⁷, A. Danilina³⁸, P. d’Argent⁴⁷, A. Davis⁶¹, O. De Aguiar Francisco⁴⁷, K. De Bruyn⁴⁷, S. De Capua⁶¹, M. De Cian⁴⁸, J.M. De Miranda¹, L. De Paula², M. De Serio^{18,d}, D. De Simone⁴⁹, P. De Simone²², J.A. de Vries⁷⁷, C.T. Dean⁶⁶, W. Dean⁸², D. Decamp⁸, L. Del Buono¹², B. Delaney⁵⁴, H.-P. Dembinski¹⁴, A. Dendek³⁴, X. Denis⁷², V. Denysenko⁴⁹, D. Derkach⁸⁰, O. Deschamps⁹, F. Desse¹¹, F. Dettori^{26,f}, B. Dey⁷, A. Di Canto⁴⁷, P. Di Nezza²², S. Didenko⁷⁹, H. Dijkstra⁴⁷, V. Dobishuk⁵¹, A.M. Donohoe¹⁷, F. Dordei²⁶, M. Dorigo^{28,x}, A.C. dos Reis¹, L. Douglas⁵⁸, A. Dovbnya⁵⁰, A.G. Downes⁸, K. Dreimanis⁵⁹, M.W. Dudek³³, L. Dufour⁴⁷, P. Durante⁴⁷, J.M. Durham⁶⁶, D. Dutta⁶¹, M. Dziewiecki¹⁶, A. Dziurda³³, A. Dzyuba³⁷, S. Easo⁵⁶, U. Egede⁶⁹, V. Egorychev³⁸, S. Eidelman^{42,w}, S. Eisenhardt⁵⁷, S. Ek-In⁴⁸, L. Eklund⁵⁸, S. Ely⁶⁷, A. Ene³⁶, E. Epple⁶⁶, S. Escher¹³, J. Eschle⁴⁹, S. Esen³¹, T. Evans⁴⁷, A. Falabella¹⁹, J. Fan³, Y. Fan⁵, B. Fang⁷², N. Farley⁵², S. Farry⁵⁹, D. Fazzini¹¹, P. Fedin³⁸, M. Féo⁴⁷, P. Fernandez Declara⁴⁷, A. Fernandez Prieto⁴⁵, F. Ferrari^{19,e}, L. Ferreira Lopes⁴⁸, F. Ferreira Rodrigues², S. Ferreres Sole³¹, M. Ferrillo⁴⁹, M. Ferro-Luzzi⁴⁷, S. Filippov⁴⁰, R.A. Fini¹⁸, M. Fiorini^{20,g}, M. Firlej³⁴, K.M. Fischer⁶², C. Fitzpatrick⁶¹, T. Fiutowski³⁴, F. Fleuret^{11,b}, M. Fontana⁴⁷, F. Fontanelli^{23,h}, R. Forty⁴⁷, V. Franco Lima⁵⁹,

M. Franco Sevilla⁶⁵, M. Frank⁴⁷, E. Franzoso²⁰, G. Frau¹⁶, C. Frei⁴⁷, D.A. Friday⁵⁸, J. Fu^{25,p},
Q. Fuehring¹⁴, W. Funk⁴⁷, E. Gabriel³¹, T. Gaintseva⁴¹, A. Gallas Torreira⁴⁵, D. Galli^{19,e},
S. Gallorini²⁷, S. Gambetta⁵⁷, Y. Gan³, M. Gandelman², P. Gandini²⁵, Y. Gao⁴, M. Garau²⁶,
L.M. Garcia Martin⁴⁶, P. Garcia Moreno⁴⁴, J. García Pardiñas⁴⁹, B. Garcia Plana⁴⁵,
F.A. Garcia Rosales¹¹, L. Garrido⁴⁴, D. Gascon⁴⁴, C. Gaspar⁴⁷, R.E. Geertsema³¹, D. Gerick¹⁶,
L.L. Gerken¹⁴, E. Gersabeck⁶¹, M. Gersabeck⁶¹, T. Gershon⁵⁵, D. Gerstel¹⁰, Ph. Ghez⁸,
V. Gibson⁵⁴, A. Gioventù⁴⁵, P. Gironella Gironell⁴⁴, L. Giubega³⁶, C. Giugliano^{20,g},
K. Gizdov⁵⁷, V.V. Gligorov¹², C. Göbel⁷⁰, E. Golobardes^{44,l}, D. Golubkov³⁸, A. Golutvin^{60,79},
A. Gomes^{1,a}, S. Gomez Fernandez⁴⁴, M. Goncerz³³, P. Gorbounov³⁸, I.V. Gorelov³⁹,
C. Gotti^{24,i}, E. Govorkova³¹, J.P. Grabowski¹⁶, R. Graciani Diaz⁴⁴, T. Grammatico¹²,
L.A. Granado Cardoso⁴⁷, E. Graugés⁴⁴, E. Graverini⁴⁸, G. Graziani²¹, A. Grecu³⁶,
L.M. Greeven³¹, P. Griffith^{20,g}, L. Grillo⁶¹, L. Gruber⁴⁷, B.R. Gruberg Cazon⁶², C. Gu³,
M. Guarise²⁰, P. A. Günther¹⁶, E. Gushchin⁴⁰, A. Guth¹³, Yu. Guz^{43,47}, T. Gys⁴⁷,
T. Hadavizadeh⁶⁹, G. Haefeli⁴⁸, C. Haen⁴⁷, S.C. Haines⁵⁴, P.M. Hamilton⁶⁵, Q. Han⁷, X. Han¹⁶,
T.H. Hancock⁶², S. Hansmann-Menzemer¹⁶, N. Harnew⁶², T. Harrison⁵⁹, R. Hart³¹, C. Hasse⁴⁷,
M. Hatch⁴⁷, J. He⁵, M. Hecker⁶⁰, K. Heijhoff³¹, K. Heinicke¹⁴, A.M. Hennequin⁴⁷,
K. Hennessy⁵⁹, L. Henry^{25,46}, J. Heuel¹³, A. Hicheur⁶⁸, D. Hill⁶², M. Hilton⁶¹, S.E. Hollitt¹⁴,
P.H. Hopchev⁴⁸, J. Hu¹⁶, J. Hu⁷¹, W. Hu⁷, W. Huang⁵, W. Hulsbergen³¹, T. Humair⁶⁰,
R.J. Hunter⁵⁵, M. Hushchyn⁸⁰, D. Hutchcroft⁵⁹, D. Hynds³¹, P. Ibis¹⁴, M. Idzik³⁴, D. Ilin³⁷,
P. Ilten⁵², A. Inglessi³⁷, K. Ivshin³⁷, R. Jacobsson⁴⁷, S. Jakobsen⁴⁷, E. Jans³¹, B.K. Jashal⁴⁶,
A. Jawahery⁶⁵, V. Jevtic¹⁴, F. Jiang³, M. John⁶², D. Johnson⁴⁷, C.R. Jones⁵⁴, T.P. Jones⁵⁵,
B. Jost⁴⁷, N. Jurik⁶², S. Kandybei⁵⁰, Y. Kang³, M. Karacson⁴⁷, J.M. Kariuki⁵³, N. Kazeev⁸⁰,
M. Kecke¹⁶, F. Keizer^{54,47}, M. Kelsey⁶⁷, M. Kenzie⁵⁵, T. Ketel³², B. Khanji⁴⁷, A. Kharisova⁸¹,
S. Kholodenko⁴³, K.E. Kim⁶⁷, T. Kirn¹³, V.S. Kirsebom⁴⁸, O. Kitouni⁶³, S. Klaver²²,
K. Klimaszewski³⁵, S. Koliiev⁵¹, A. Kondybayeva⁷⁹, A. Konoplyannikov³⁸, P. Kopciwicz³⁴,
R. Kopečna¹⁶, P. Koppenburg³¹, M. Korolev³⁹, I. Kostiuk^{31,51}, O. Kot⁵¹, S. Kotriakhova³⁷,
P. Kravchenko³⁷, L. Kravchuk⁴⁰, R.D. Krawczyk⁴⁷, M. Kreps⁵⁵, F. Kress⁶⁰, S. Kretschmar¹³,
P. Krokovny^{42,w}, W. Krupa³⁴, W. Krzemien³⁵, W. Kucewicz^{84,33,k}, M. Kucharczyk³³,
V. Kudryavtsev^{42,w}, H.S. Kuindersma³¹, G.J. Kunde⁶⁶, T. Kvaratskheliya³⁸, D. Lacarrere⁴⁷,
G. Lafferty⁶¹, A. Lai²⁶, A. Lampis²⁶, D. Lancierini⁴⁹, J.J. Lane⁶¹, R. Lane⁵³, G. Lanfranchi²²,
C. Langenbruch¹³, J. Langer¹⁴, O. Lantwin^{49,79}, T. Latham⁵⁵, F. Lazzari^{28,u}, R. Le Gac¹⁰,
S.H. Lee⁸², R. Lefèvre⁹, A. Leflat^{39,47}, S. Legotin⁷⁹, O. Leroy¹⁰, T. Lesiak³³, B. Leverington¹⁶,
H. Li⁷¹, L. Li⁶², P. Li¹⁶, X. Li⁶⁶, Y. Li⁶, Y. Li⁶, Z. Li⁶⁷, X. Liang⁶⁷, T. Lin⁶⁰, R. Lindner⁴⁷,
V. Lisovskyi¹⁴, R. Litvinov²⁶, G. Liu⁷¹, H. Liu⁵, S. Liu⁶, X. Liu³, A. Loi²⁶, J. Lomba Castro⁴⁵,
I. Longstaff⁵⁸, J.H. Lopes², G. Loustau⁴⁹, G.H. Lovell⁵⁴, Y. Lu⁶, D. Lucchesi^{27,n}, S. Luchuk⁴⁰,
M. Lucio Martinez³¹, V. Lukashenko³¹, Y. Luo³, A. Lupato⁶¹, E. Luppi^{20,g}, O. Lupton⁵⁵,
A. Lusiani^{28,s}, X. Lyu⁵, L. Ma⁶, S. Maccolini^{19,e}, F. Machefer¹¹, F. Maciuc³⁶, V. Macko⁴⁸,
P. Mackowiak¹⁴, S. Maddrell-Mander⁵³, L.R. Madhan Mohan⁵³, O. Maev³⁷, A. Maevskiy⁸⁰,
D. Maisuzenko³⁷, M.W. Majewski³⁴, S. Malde⁶², B. Malecki⁴⁷, A. Malinin⁷⁸, T. Maltsev^{42,w},
H. Malygina¹⁶, G. Manca^{26,f}, G. Mancinelli¹⁰, R. Manera Escalero⁴⁴, D. Manuzzi^{19,e},
D. Marangotto^{25,p}, J. Maratas^{9,v}, J.F. Marchand⁸, U. Marconi¹⁹, S. Mariani^{21,21,47},
C. Marin Benito¹¹, M. Marinangeli⁴⁸, P. Marino⁴⁸, J. Marks¹⁶, P.J. Marshall⁵⁹, G. Martellotti³⁰,
L. Martinazzoli⁴⁷, M. Martinelli^{24,i}, D. Martinez Santos⁴⁵, F. Martinez Vidal⁴⁶, A. Massafferri¹,
M. Materok¹³, R. Matev⁴⁷, A. Mathad⁴⁹, Z. Mathe⁴⁷, V. Matiunin³⁸, C. Matteuzzi²⁴,
K.R. Mattioli⁸², A. Mauri⁴⁹, E. Maurice^{83,11,b}, J. Mauricio⁴⁴, M. Mazurek³⁵, M. McCann⁶⁰,
L. McConnell¹⁷, T.H. Mcgrath⁶¹, A. McNab⁶¹, R. McNulty¹⁷, J.V. Mead⁵⁹, B. Meadows⁶⁴,
C. Meaux¹⁰, G. Meier¹⁴, N. Meinert⁷⁵, D. Melnychuk³⁵, S. Meloni^{24,i}, M. Merk^{31,77}, A. Merli²⁵,
L. Meyer Garcia², M. Mikhasenko⁴⁷, D.A. Milanese⁷³, E. Millard⁵⁵, M.-N. Minard⁸,
L. Minzoni^{20,g}, S.E. Mitchell⁵⁷, B. Mitreska⁶¹, D.S. Mitzel⁴⁷, A. Mödden¹⁴, R.A. Mohammed⁶²,
R.D. Moise⁶⁰, T. Mombächer¹⁴, I.A. Monroy⁷³, S. Monteil⁹, M. Morandin²⁷, G. Morello²²,

M.J. Morello^{28,s}, J. Moron³⁴, A.B. Morris⁷⁴, A.G. Morris⁵⁵, R. Mountain⁶⁷, H. Mu³,
F. Muheim⁵⁷, M. Mukherjee⁷, M. Mulder⁴⁷, D. Müller⁴⁷, K. Müller⁴⁹, C.H. Murphy⁶²,
D. Murray⁶¹, P. Muzzetto²⁶, P. Naik⁵³, T. Nakada⁴⁸, R. Nandakumar⁵⁶, T. Nanut⁴⁸,
I. Nasteva², M. Needham⁵⁷, I. Neri^{20,g}, N. Neri^{25,p}, S. Neubert⁷⁴, N. Neufeld⁴⁷, R. Newcombe⁶⁰,
T.D. Nguyen⁴⁸, C. Nguyen-Mau^{48,m}, E.M. Niel¹¹, S. Nieswand¹³, N. Nikitin³⁹, N.S. Nolte⁴⁷,
C. Nunez⁸², A. Oblakowska-Mucha³⁴, V. Obraztsov⁴³, S. Ogilvy⁵⁸, D.P. O’Hanlon⁵³,
R. Oldeman^{26,f}, C.J.G. Onderwater⁷⁶, J. D. Osborn⁸², A. Ossowska³³, J.M. Otalora Goicochea²,
T. Ovsianikova³⁸, P. Owen⁴⁹, A. Oyanguren⁴⁶, B. Pagare⁵⁵, P.R. Pais⁴⁷, T. Pajero^{28,47,s},
A. Palano¹⁸, M. Palutan²², Y. Pan⁶¹, G. Panshin⁸¹, A. Papanestis⁵⁶, M. Pappagallo⁵⁷,
L.L. Pappalardo^{20,g}, C. Pappenheimer⁶⁴, W. Parker⁶⁵, C. Parkes⁶¹, C.J. Parkinson⁴⁵,
B. Passalacqua²⁰, G. Passaleva^{21,47}, A. Pastore¹⁸, M. Patel⁶⁰, C. Patrignani^{19,e}, A. Pearce⁴⁷,
A. Pellegrino³¹, M. Pepe Altarelli⁴⁷, S. Perazzini¹⁹, D. Pereima³⁸, P. Perret⁹, K. Petridis⁵³,
A. Petrolini^{23,h}, A. Petrov⁷⁸, S. Petrucci⁵⁷, M. Petruzzo²⁵, A. Philippov⁴¹, L. Pica²⁸,
B. Pietrzyk⁸, G. Pietrzyk⁴⁸, M. Pili⁶², D. Pinci³⁰, J. Pinzino⁴⁷, F. Pisani⁴⁷, A. Piucci¹⁶, Resmi
P.K¹⁰, V. Placinta³⁶, S. Playfer⁵⁷, J. Plews⁵², M. Plo Casasus⁴⁵, F. Polci¹², M. Poli Lener²²,
M. Poliakova⁶⁷, A. Poluektov¹⁰, N. Polukhina^{79,c}, I. Polyakov⁶⁷, E. Polcarpo², G.J. Pomery⁵³,
S. Ponce⁴⁷, A. Popov⁴³, D. Popov^{5,47}, S. Popov⁴¹, S. Poslavskii⁴³, K. Prasanth³³,
L. Promberger⁴⁷, C. Prouve⁴⁵, V. Pugatch⁵¹, A. Puig Navarro⁴⁹, H. Pullen⁶², G. Punzi^{28,o},
W. Qian⁵, J. Qin⁵, R. Quagliani¹², B. Quintana⁸, N.V. Raab¹⁷, R.I. Rabadan Trejo¹⁰,
B. Rachwal³⁴, J.H. Rademacker⁵³, M. Rama²⁸, M. Ramos Pernas⁴⁵, M.S. Rangel²,
F. Ratnikov^{41,80}, G. Raven³², M. Reboud⁸, F. Redi⁴⁸, F. Reiss¹², C. Remon Alepuz⁴⁶, Z. Ren³,
V. Renaudin⁶², R. Ribatti²⁸, S. Ricciardi⁵⁶, D.S. Richards⁵⁶, K. Rinnert⁵⁹, P. Robbe¹¹,
A. Robert¹², G. Robertson⁵⁷, A.B. Rodrigues⁴⁸, E. Rodrigues⁵⁹, J.A. Rodriguez Lopez⁷³,
M. Roehrken⁴⁷, A. Rollings⁶², P. Roloff⁴⁷, V. Romanovskiy⁴³, M. Romero Lamas⁴⁵,
A. Romero Vidal⁴⁵, J.D. Roth⁸², M. Rotondo²², M.S. Rudolph⁶⁷, T. Ruf⁴⁷, J. Ruiz Vidal⁴⁶,
A. Ryzhikov⁸⁰, J. Ryzka³⁴, J.J. Saborido Silva⁴⁵, N. Sagidova³⁷, N. Sahoo⁵⁵, B. Saitta^{26,f},
C. Sanchez Gras³¹, C. Sanchez Mayordomo⁴⁶, R. Santacesaria³⁰, C. Santamarina Rios⁴⁵,
M. Santimaria²², E. Santovetti^{29,j}, D. Saranin⁷⁹, G. Sarpis⁶¹, M. Sarpis⁷⁴, A. Sarti³⁰,
C. Satriano^{30,r}, A. Satta²⁹, M. Saur⁵, D. Savrina^{38,39}, H. Sazak⁹, L.G. Scantlebury Smead⁶²,
S. Schael¹³, M. Schellenberg¹⁴, M. Schiller⁵⁸, H. Schindler⁴⁷, M. Schmelling¹⁵, T. Schmelzer¹⁴,
B. Schmidt⁴⁷, O. Schneider⁴⁸, A. Schopper⁴⁷, H.F. Schreiner⁶⁴, M. Schubiger³¹, S. Schulte⁴⁸,
M.H. Schune¹¹, R. Schwemmer⁴⁷, B. Sciascia²², A. Sciubba²², S. Sellam⁶⁸, A. Semennikov³⁸,
A. Sergi^{52,47}, N. Serra⁴⁹, J. Serrano¹⁰, L. Sestini²⁷, A. Seuthe¹⁴, P. Seyfert⁴⁷, D.M. Shangase⁸²,
M. Shapkin⁴³, I. Shchemerov⁷⁹, L. Shchutska⁴⁸, T. Shears⁵⁹, L. Shekhtman^{42,w},
V. Shevchenko⁷⁸, E.B. Shields^{24,i}, E. Shmanin⁷⁹, J.D. Shupperd⁶⁷, B.G. Siddi²⁰,
R. Silva Coutinho⁴⁹, L. Silva de Oliveira², G. Simi²⁷, S. Simone^{18,d}, I. Skiba^{20,g}, N. Skidmore⁷⁴,
T. Skwarnicki⁶⁷, M.W. Slater⁵², J.C. Smallwood⁶², J.G. Smeaton⁵⁴, A. Smetkina³⁸, E. Smith¹³,
M. Smith⁶⁰, A. Snoch³¹, M. Soares¹⁹, L. Soares Lavra⁹, M.D. Sokoloff⁶⁴, F.J.P. Soler⁵⁸,
A. Solovev³⁷, I. Solovyev³⁷, F.L. Souza De Almeida², B. Souza De Paula², B. Spaan¹⁴,
E. Spadaro Norella^{25,p}, P. Spradlin⁵⁸, F. Stagni⁴⁷, M. Stahl⁶⁴, S. Stahl⁴⁷, P. Stefko⁴⁸,
O. Steinkamp^{49,79}, S. Stemmler¹⁶, O. Stenyakin⁴³, H. Stevens¹⁴, S. Stone⁶⁷, S. Stracka²⁸,
M.E. Stramaglia⁴⁸, M. Straticiu³⁶, D. Strelakina⁷⁹, S. Strokov⁸¹, F. Suljik⁶², J. Sun²⁶, L. Sun⁷²,
Y. Sun⁶⁵, P. Svihra⁶¹, P.N. Swallow⁵², K. Swientek³⁴, A. Szabelski³⁵, T. Szumlak³⁴,
M. Szymanski⁴⁷, S. Taneja⁶¹, Z. Tang³, T. Tekampe¹⁴, F. Teubert⁴⁷, E. Thomas⁴⁷,
K.A. Thomson⁵⁹, M.J. Tilley⁶⁰, V. Tisserand⁹, S. T’Jampens⁸, M. Tobin⁶, S. Tolk⁴⁷,
L. Tomassetti^{20,g}, D. Torres Machado¹, D.Y. Tou¹², M. Traill⁵⁸, M.T. Tran⁴⁸, E. Trifonova⁷⁹,
C. Trippl⁴⁸, A. Tsaregorodtsev¹⁰, G. Tuci^{28,o}, A. Tully⁴⁸, N. Tuning³¹, A. Ukleja³⁵,
D.J. Unverzagt¹⁶, A. Usachov³¹, A. Ustyuzhanin^{41,80}, U. Uwer¹⁶, A. Vagner⁸¹, V. Vagnoni¹⁹,
A. Valassi⁴⁷, G. Valenti¹⁹, M. van Beuzekom³¹, H. Van Hecke⁶⁶, E. van Herwijnen⁷⁹,
C.B. Van Hulse¹⁷, M. van Veghel⁷⁶, R. Vazquez Gomez⁴⁵, P. Vazquez Regueiro⁴⁵,

C. Vázquez Sierra³¹, S. Vecchi²⁰, J.J. Velthuis⁵³, M. Veltri^{21,q}, A. Venkateswaran⁶⁷,
M. Veronesi³¹, M. Vesterinen⁵⁵, D. Vieira⁶⁴, M. Vieites Diaz⁴⁸, H. Viemann⁷⁵,
X. Vilasis-Cardona⁴⁴, E. Vilella Figueras⁵⁹, P. Vincent¹², G. Vitali²⁸, A. Vitkovskiy³¹,
A. Vollhardt⁴⁹, D. Vom Bruch¹², A. Vorobyev³⁷, V. Vorobyev^{42,w}, N. Voropaev³⁷, R. Waldi⁷⁵,
J. Walsh²⁸, C. Wang¹⁶, J. Wang³, J. Wang⁷², J. Wang⁴, J. Wang⁶, M. Wang³, R. Wang⁵³,
Y. Wang⁷, Z. Wang⁴⁹, D.R. Ward⁵⁴, H.M. Wark⁵⁹, N.K. Watson⁵², S.G. Weber¹²,
D. Websdale⁶⁰, C. Weisser⁶³, B.D.C. Westhenry⁵³, D.J. White⁶¹, M. Whitehead⁵³,
D. Wiedner¹⁴, G. Wilkinson⁶², M. Wilkinson⁶⁷, I. Williams⁵⁴, M. Williams^{63,69},
M.R.J. Williams⁶¹, F.F. Wilson⁵⁶, M. Winn¹¹, W. Wislicki³⁵, M. Witek³³, L. Witola¹⁶,
G. Wormser¹¹, S.A. Wotton⁵⁴, H. Wu⁶⁷, K. Wyllie⁴⁷, Z. Xiang⁵, D. Xiao⁷, Y. Xie⁷, H. Xing⁷¹,
A. Xu⁴, J. Xu⁵, L. Xu³, M. Xu⁷, Q. Xu⁵, Z. Xu⁴, D. Yang³, Y. Yang⁵, Z. Yang³, Z. Yang⁶⁵,
Y. Yao⁶⁷, L.E. Yeomans⁵⁹, H. Yin⁷, J. Yu⁷, X. Yuan⁶⁷, O. Yushchenko⁴³, K.A. Zarebski⁵²,
M. Zavertyaev^{15,c}, M. Zdybal³³, O. Zenaiev⁴⁷, M. Zeng³, D. Zhang⁷, L. Zhang³, S. Zhang⁴,
Y. Zhang⁴⁷, A. Zhelezov¹⁶, Y. Zheng⁵, X. Zhou⁵, Y. Zhou⁵, X. Zhu³, V. Zhukov^{13,39},
J.B. Zonneveld⁵⁷, S. Zucchelli^{19,e}, D. Zuliani²⁷, G. Zunica⁶¹.

¹ *Centro Brasileiro de Pesquisas Físicas (CBPF), Rio de Janeiro, Brazil*

² *Universidade Federal do Rio de Janeiro (UFRJ), Rio de Janeiro, Brazil*

³ *Center for High Energy Physics, Tsinghua University, Beijing, China*

⁴ *School of Physics State Key Laboratory of Nuclear Physics and Technology, Peking University, Beijing, China*

⁵ *University of Chinese Academy of Sciences, Beijing, China*

⁶ *Institute Of High Energy Physics (IHEP), Beijing, China*

⁷ *Institute of Particle Physics, Central China Normal University, Wuhan, Hubei, China*

⁸ *Univ. Grenoble Alpes, Univ. Savoie Mont Blanc, CNRS, IN2P3-LAPP, Annecy, France*

⁹ *Université Clermont Auvergne, CNRS/IN2P3, LPC, Clermont-Ferrand, France*

¹⁰ *Aix Marseille Univ, CNRS/IN2P3, CPPM, Marseille, France*

¹¹ *Université Paris-Saclay, CNRS/IN2P3, IJCLab, Orsay, France*

¹² *LPNHE, Sorbonne Université, Paris Diderot Sorbonne Paris Cité, CNRS/IN2P3, Paris, France*

¹³ *I. Physikalisches Institut, RWTH Aachen University, Aachen, Germany*

¹⁴ *Fakultät Physik, Technische Universität Dortmund, Dortmund, Germany*

¹⁵ *Max-Planck-Institut für Kernphysik (MPIK), Heidelberg, Germany*

¹⁶ *Physikalisches Institut, Ruprecht-Karls-Universität Heidelberg, Heidelberg, Germany*

¹⁷ *School of Physics, University College Dublin, Dublin, Ireland*

¹⁸ *INFN Sezione di Bari, Bari, Italy*

¹⁹ *INFN Sezione di Bologna, Bologna, Italy*

²⁰ *INFN Sezione di Ferrara, Ferrara, Italy*

²¹ *INFN Sezione di Firenze, Firenze, Italy*

²² *INFN Laboratori Nazionali di Frascati, Frascati, Italy*

²³ *INFN Sezione di Genova, Genova, Italy*

²⁴ *INFN Sezione di Milano-Bicocca, Milano, Italy*

²⁵ *INFN Sezione di Milano, Milano, Italy*

²⁶ *INFN Sezione di Cagliari, Monserrato, Italy*

²⁷ *Università degli Studi di Padova, Università e INFN, Padova, Padova, Italy*

²⁸ *INFN Sezione di Pisa, Pisa, Italy*

²⁹ *INFN Sezione di Roma Tor Vergata, Roma, Italy*

³⁰ *INFN Sezione di Roma La Sapienza, Roma, Italy*

³¹ *Nikhef National Institute for Subatomic Physics, Amsterdam, Netherlands*

³² *Nikhef National Institute for Subatomic Physics and VU University Amsterdam, Amsterdam, Netherlands*

³³ *Henryk Niewodniczanski Institute of Nuclear Physics Polish Academy of Sciences, Kraków, Poland*

³⁴ *AGH - University of Science and Technology, Faculty of Physics and Applied Computer Science, Kraków, Poland*

³⁵ *National Center for Nuclear Research (NCBJ), Warsaw, Poland*

³⁶ *Horia Hulubei National Institute of Physics and Nuclear Engineering, Bucharest-Magurele, Romania*

- ³⁷ Petersburg Nuclear Physics Institute NRC Kurchatov Institute (PNPI NRC KI), Gatchina, Russia
- ³⁸ Institute of Theoretical and Experimental Physics NRC Kurchatov Institute (ITEP NRC KI), Moscow, Russia, Moscow, Russia
- ³⁹ Institute of Nuclear Physics, Moscow State University (SINP MSU), Moscow, Russia
- ⁴⁰ Institute for Nuclear Research of the Russian Academy of Sciences (INR RAS), Moscow, Russia
- ⁴¹ Yandex School of Data Analysis, Moscow, Russia
- ⁴² Budker Institute of Nuclear Physics (SB RAS), Novosibirsk, Russia
- ⁴³ Institute for High Energy Physics NRC Kurchatov Institute (IHEP NRC KI), Protvino, Russia, Protvino, Russia
- ⁴⁴ ICCUB, Universitat de Barcelona, Barcelona, Spain
- ⁴⁵ Instituto Galego de Física de Altas Enerxías (IGFAE), Universidade de Santiago de Compostela, Santiago de Compostela, Spain
- ⁴⁶ Instituto de Física Corpuscular, Centro Mixto Universidad de Valencia - CSIC, Valencia, Spain
- ⁴⁷ European Organization for Nuclear Research (CERN), Geneva, Switzerland
- ⁴⁸ Institute of Physics, Ecole Polytechnique Fédérale de Lausanne (EPFL), Lausanne, Switzerland
- ⁴⁹ Physik-Institut, Universität Zürich, Zürich, Switzerland
- ⁵⁰ NSC Kharkiv Institute of Physics and Technology (NSC KIPT), Kharkiv, Ukraine
- ⁵¹ Institute for Nuclear Research of the National Academy of Sciences (KINR), Kyiv, Ukraine
- ⁵² University of Birmingham, Birmingham, United Kingdom
- ⁵³ H.H. Wills Physics Laboratory, University of Bristol, Bristol, United Kingdom
- ⁵⁴ Cavendish Laboratory, University of Cambridge, Cambridge, United Kingdom
- ⁵⁵ Department of Physics, University of Warwick, Coventry, United Kingdom
- ⁵⁶ STFC Rutherford Appleton Laboratory, Didcot, United Kingdom
- ⁵⁷ School of Physics and Astronomy, University of Edinburgh, Edinburgh, United Kingdom
- ⁵⁸ School of Physics and Astronomy, University of Glasgow, Glasgow, United Kingdom
- ⁵⁹ Oliver Lodge Laboratory, University of Liverpool, Liverpool, United Kingdom
- ⁶⁰ Imperial College London, London, United Kingdom
- ⁶¹ Department of Physics and Astronomy, University of Manchester, Manchester, United Kingdom
- ⁶² Department of Physics, University of Oxford, Oxford, United Kingdom
- ⁶³ Massachusetts Institute of Technology, Cambridge, MA, United States
- ⁶⁴ University of Cincinnati, Cincinnati, OH, United States
- ⁶⁵ University of Maryland, College Park, MD, United States
- ⁶⁶ Los Alamos National Laboratory (LANL), Los Alamos, United States
- ⁶⁷ Syracuse University, Syracuse, NY, United States
- ⁶⁸ Laboratory of Mathematical and Subatomic Physics, Constantine, Algeria, associated to ²
- ⁶⁹ School of Physics and Astronomy, Monash University, Melbourne, Australia, associated to ⁵⁵
- ⁷⁰ Pontifícia Universidade Católica do Rio de Janeiro (PUC-Rio), Rio de Janeiro, Brazil, associated to ²
- ⁷¹ Guangdong Provincial Key Laboratory of Nuclear Science, Institute of Quantum Matter, South China Normal University, Guangzhou, China, associated to ³
- ⁷² School of Physics and Technology, Wuhan University, Wuhan, China, associated to ³
- ⁷³ Departamento de Física, Universidad Nacional de Colombia, Bogota, Colombia, associated to ¹²
- ⁷⁴ Universität Bonn - Helmholtz-Institut für Strahlen und Kernphysik, Bonn, Germany, associated to ¹⁶
- ⁷⁵ Institut für Physik, Universität Rostock, Rostock, Germany, associated to ¹⁶
- ⁷⁶ Van Swinderen Institute, University of Groningen, Groningen, Netherlands, associated to ³¹
- ⁷⁷ Universiteit Maastricht, Maastricht, Netherlands, associated to ³¹
- ⁷⁸ National Research Centre Kurchatov Institute, Moscow, Russia, associated to ³⁸
- ⁷⁹ National University of Science and Technology "MISIS", Moscow, Russia, associated to ³⁸
- ⁸⁰ National Research University Higher School of Economics, Moscow, Russia, associated to ⁴¹
- ⁸¹ National Research Tomsk Polytechnic University, Tomsk, Russia, associated to ³⁸
- ⁸² University of Michigan, Ann Arbor, United States, associated to ⁶⁷
- ⁸³ Laboratoire Leprince-Ringuet, Palaiseau, France
- ⁸⁴ AGH - University of Science and Technology, Faculty of Computer Science, Electronics and Telecommunications, Kraków, Poland

^a Universidade Federal do Triângulo Mineiro (UFTM), Uberaba-MG, Brazil

^b Laboratoire Leprince-Ringuet, Palaiseau, France

^c P.N. Lebedev Physical Institute, Russian Academy of Science (LPI RAS), Moscow, Russia

- ^d *Università di Bari, Bari, Italy*
- ^e *Università di Bologna, Bologna, Italy*
- ^f *Università di Cagliari, Cagliari, Italy*
- ^g *Università di Ferrara, Ferrara, Italy*
- ^h *Università di Genova, Genova, Italy*
- ⁱ *Università di Milano Bicocca, Milano, Italy*
- ^j *Università di Roma Tor Vergata, Roma, Italy*
- ^k *AGH - University of Science and Technology, Faculty of Computer Science, Electronics and Telecommunications, Kraków, Poland*
- ^l *DS4DS, La Salle, Universitat Ramon Llull, Barcelona, Spain*
- ^m *Hanoi University of Science, Hanoi, Vietnam*
- ⁿ *Università di Padova, Padova, Italy*
- ^o *Università di Pisa, Pisa, Italy*
- ^p *Università degli Studi di Milano, Milano, Italy*
- ^q *Università di Urbino, Urbino, Italy*
- ^r *Università della Basilicata, Potenza, Italy*
- ^s *Scuola Normale Superiore, Pisa, Italy*
- ^t *Università di Modena e Reggio Emilia, Modena, Italy*
- ^u *Università di Siena, Siena, Italy*
- ^v *MSU - Iligan Institute of Technology (MSU-IIT), Iligan, Philippines*
- ^w *Novosibirsk State University, Novosibirsk, Russia*
- ^x *INFN Sezione di Trieste, Trieste, Italy*
- ^y *Universidad Nacional Autónoma de Honduras, Tegucigalpa, Honduras*